Journal of Quantitative Spectroscopy & Radiative Transfer ■ (■■■■) ■■■–■■■

Contents lists available at ScienceDirect

Journal of Quantitative Spectroscopy & Radiative Transfer

journal homepage: www.elsevier.com/locate/jqsrt

Room temperature linelists for CO_2 asymmetric isotopologues with *ab initio* computed intensities

Emil J. Zak [a], Jonathan Tennyson [a,*], Oleg L. Polyansky [a,b], Lorenzo Lodi [a], Nikolay F. Zobov [b], Sergei A. Tashkun [c], Valery I. Perevalov [c]

[a] Department of Physics and Astronomy, University College London, London WC1E 6BT, UK
[b] Institute of Applied Physics, Russian Academy of Sciences, Ulyanov Street 46, Nizhny Novgorod 603950, Russia
[c] V.E. Zuev Institute of Atmospheric Optics, SB RAS, 1, Academician Zuev Square, Tomsk 634021, Russia

ARTICLE INFO

Article history:
Received 1 December 2016
Received in revised form
26 January 2017
Accepted 29 January 2017

ABSTRACT

The present paper reports room temperature line lists for six asymmetric isotopologues of carbon dioxide: $^{16}O^{12}C^{18}O$ (628), $^{16}O^{12}C^{17}O$ (627), $^{16}O^{13}C^{18}O$ (638),$^{16}O^{13}C^{17}O$ (637), $^{17}O^{12}C^{18}O$ (728) and $^{17}O^{13}C^{18}O$ (738), covering the range 0–8000 cm^{-1}. Variational rotation-vibration wavefunctions and energy levels are computed using the DVR3D software suite and a high quality semi-empirical potential energy surface (PES), followed by computation of intensities using an *ab initio* dipole moment surface (DMS). A theoretical procedure for quantifying sensitivity of line intensities to minor distortions of the PES/DMS renders our theoretical model as critically evaluated. Several recent high quality measurements and theoretical approaches are discussed to provide a benchmark of our results against the most accurate available data. Indeed, the thesis of transferability of accuracy among different isotopologues with the use of mass-independent PES is supported by several examples. Thereby, we conclude that the majority of line intensities for strong bands are predicted with sub-percent accuracy. Accurate line positions are generated using an effective Hamiltonian, constructed from the latest experiments. This study completes the list of relevant isotopologues of carbon dioxide; these line lists are available to remote sensing studies and inclusion in databases.

1. Introduction

Recently we reported room temperature line lists for the main $^{12}C^{16}O_2$ [1] and other symmetric [2] isotopologues of carbon dioxide. These studies covered the 0–8000 cm^{-1} spectral region and 10^{-30} cm/molecule cut-off on transition intensities at 296 K. The purpose of the line lists provided was to deliver as complete as possible description of the infra-red spectra of CO_2 with highly accurate line intensities. These intensities have been proven to display sub-percent accuracy for several strong bands of the main isotopologue [3–7]. Tentative indication of similar accuracy has been recently reported for the 30013–00001 band of less abundant symmetric 636 isotopologue [2,6]. Together with our reliability analysis of the transition intensities on a purely theoretical basis, we presented semi-empirical line positions taken from the effective Hamiltonian (EH) calculations. This constituted a comprehensive study, readily applicable to numerous problems, such as determination of isotopic ratios of carbon in geophysical samples, quantification of ^{14}C in fossil fuels or concentration measurements of carbon dioxide by ground based and space missions.

A number of spectroscopic measurements on carbon dioxide require simultaneous knowledge of accurate line positions and line intensities for both its most abundant and rare isotopologues. A primary example of such situation is experimental retrieval of the concentration of $^{14}CO_2$ in an environmental sample. The P(20) line of the asymmetric stretching fundamental ν_3 band usually utilized for this purpose nearly overlaps with the P(19) line of a hot band originating from $^{13}CO_2$. The quality of the elucidated concentration is therefore sensitive to the accuracy of both lines.

Another application that requires *a priori* knowledge of line intensities of multiple isotopologues at the same time is determination of $^{13}C/^{12}C$ and $^{16}O/^{17}O/^{18}O$ ratios. These ratios remain crucial for modelling the Earth's geophysical processes, but also for example, in investigating processes of formation of radiation fields in the Martian atmosphere, which is 96% rich in carbon dioxide [8]. The low natural abundances of ^{13}C, ^{17}O and ^{18}O usually inhibit high accuracy measurements of integral intensities on these CO_2 species due in part to spectral congestion from more abundant isotopologues. Only recently, studies by Jacquemart et al. [9], Borkov et al. [10,11] and Karlovets et al. [13–17] on isotopically

* Corresponding author.
E-mail address: j.tennyson@ucl.ac.uk (J. Tennyson).

http://dx.doi.org/10.1016/j.jqsrt.2017.01.037

Table 1
Summary of 13 room temperature (T=296 K) line lists of carbon dioxide from this work and our previous studies [1,2].

Isotopologue	626	636	646	727	737	828	838	628	627	637	638	728	738
ZPE[a] [cm^{-1}]	2535.92	2483.08	2436.75	2500.75	2447.50	2469.05	2415.39	2502.61	2518.35	2465.33	2449.38	2484.93	2431.48
J_{MAX}	129	119	130	99	50	101	50	118	112	99	102	99	84
SF(ortho:para)[b]	1:0	2:0	7:0	15:21	30:42	1:0	2:0	1	6	12	2	6	12
Q_{296} (This work)	286.095	576.652	2033.395	10 902.24	21 758.08	323.438	644.754	607.855	3536.724	7129.752	1223.560	3760.428	7583.400
Q_{296}(CDSD-296)[c]	286.098	576.652	N/A	10 971.90	22 129.96	323.418	652.234	607.828	3542.639	7141.561	1225.518	3766.689	7595.295
Q_{296}(Ames-296)[d]	286.094	576.644	2033.353	10 971.91	22 129.96	323.424	652.242	607.713	3542.610	7140.024	1225.270	3766.044	7593.900
Q_{296}(HITRAN)[e]	286.936	578.408	N/A	11 001.67	N/A	324.211	653.756	609.480	3552.678	7162.908	1229.084	3776.352	7615.248
Abundance[f]	0.9842	1.1057(-2)	1.0	1.3685(-7)	1.5375(-9)	3.9556(-6)	4.4440(-8)	3.9470(-3)	7.3399(-4)	8.2462(-6)	4.4345(-5)	1.4718(-6)	1.653(-8)
N(This work)[g]	162 010	68 635	41 610	6530	1501	10 441	2637	117 490	71 580	22 667	39 980	14 349	3573
N(CDSD-296)[g]	160 499	68 640	N/A	6530	1500	10 444	2635	113 122	70 692	23 815	39 979	15 140	3621
N(Ames-296)[g]	162 558	68 739	42 072	6545	1634	10 531	3050	117 744	71 639	22 704	40 034	14 529	3573
N(HITRAN2012)	160 292	68 856	N/A	5187	N/A	7070	121	114 023	71 182	2953	26 737	821	N/A
Matched[h]	160 289	68 856	N/A	5187	N/A	7069	121	110 292	71 016	2736	26 713	816	N/A

[a] Zero point energy computed with DVR3D with the Ames-1 PES.
[b] Nuclear spin statistical weights multiplied by degeneracy factor.
[c] 2015 Edition of CDSD [19];
[d] [22].
[e] TIPS-2011 [35].
[f] HITRAN2012 abundances were taken from Ref. [22].
[g] For 10^{-27} cm/molecule intensity cut-off and 10^{-30} cm/molecule after scaling by the natural abundance for the other isotopologues.
[h] UCL line list with 10^{-33} cm/molecule intensity cut-off was used in the comparison.

enriched samples have given a more detailed knowledge about the structure of weaker bands in the asymmetric isotopologues and thus improved the accuracy of the available intensities of key strong bands. Although transition frequencies are measured with satisfactory precision in this way, lack of spectral completeness remains an issue, which is partially solved by spectroscopic databases like HITRAN [18], CDSD-296 [19] or GEISA [20]. These databases, however, rely heavily on experiments which suffer from insufficiently accurate line intensities. For this reason, a self-consistent database containing high-quality spectroscopic information about both line positions and intensities for all isotopologues of CO_2 is necessary for successful and reliable retrievals. Here we provide a solution to the intensity problem in the form of line lists, which we hope, will cross-validate and update existing room temperature databases.

The 2012 release of the HITRAN database contains only a limited number of entries for the asymmetric isotopologues of carbon dioxide, leaving spectral gaps and minor inconsistencies in intensity patterns due to more than one source used for a single band. Typically, line positions used in HITRAN are at the level of accuracy not achievable with standard variational methods. In HITRAN, some line positions come from experiment but mainly they are taken from effective Hamiltonian models introduced by Tashkun and Perevalov; these models encompass all precise measurements in the form of a single coherent database and have been published independently as CDSD-296 [19].

As mentioned earlier, transition intensities are more challenging experimentally, thus only limited work has been done to obtain the level of accuracy (0.3–1% [21]) required by remote sensing missions dedicated to monitor the concentration of carbon dioxide in the Earth's atmosphere. This is, for instance, the main requirement for successful interpretation of data from the NASA Orbiting Carbon Observatory 2 (OCO-2) space mission [21].

For this purpose, *ab initio* or semi-empirical models are needed. The accuracy of such models is determined by the quality of the underlying surfaces: potential energy surface (PES) and dipole moment surface (DMS). Whereas the former is usually empirically fitted to give ro-vibrational energy levels and wavefunctions, the latter is mainly responsible for the accuracy of the transition intensities and commonly appears in *ab initio* form.

A recent theoretical attempt to model high-resolution infrared spectra of carbon dioxide has been made in the work by Huang et al. from the NASA Ames Research Center [22,23]. These authors published a semi-empirical PES named 'Ames-1' and an *ab initio* DMS. The Ames line lists constructed upon these surfaces has been proven to be very accurate for both the symmetric and asymmetric isotopologues [4,5,24,25]. This important fact supports the thesis that line intensities can be computed variationally using mass-independent PES for all isotopologues with little loss in accuracy. This relies on the non-Born-Oppenheimer corrections giving negligible, possibly mutually cancelling effects, which enter the stipulated uncertainty budget. We believe that the error introduced by neglecting non-BO effects manifests itself below the stated 1% uncertainty tolerance for line intensities. This issue has been already discussed in our previous work on the symmetric isotopologues [2].

Uncertainties in the line intensities in the HITRAN2012 database for the asymmetric isotopologues of CO_2 vary from 2% to over 20%. Whilst the majority of lines have a declared accuracy of 20% or worse, this assessment had been shown to be too pessimistic in many cases [1,2,4,5,23]. There are several recent high-quality measurements on ^{17}O and ^{18}O enriched samples of carbon dioxide [9,10,14–16,26,27], some of which give comparisons to the HITRAN2012 and Ames line lists, revealing good (usually better than 10%) overall agreement between HITRAN, Ames and the experimental line intensities; these comparisons deliver a test of

Please cite this article as: Zak EJ, et al. Room temperature linelists for CO_2 asymmetric isotopologues with *ab initio* computed intensities. J Quant Spectrosc Radiat Transfer (2017), http://dx.doi.org/10.1016/j.jqsrt.2017.01.037

consistency between the measurement and the databases. Here we use the established accuracy of the measurements and the theoretical studies to perform a critical analysis of the intensities computed using our *ab initio* dipole moment surface [1,3].

Line positions, derived from a variational approach and based on semi-empirical potential energy surface (PES), are accurate to 0.03–0.2 cm^{-1}. Although the Ames-1 line lists [22,23] show the best agreement with experiment among all variational calculations, semi-empirical approaches based on effective Hamiltonians can provide line positions with an accuracy at least one order of magnitude better [28]. On the other hand, effective Hamiltonian models strongly depend on the quality of the input data, thus the accuracy and completeness of this technique are limited by existing experiment.

The main source of errors in line intensity is DMS. In instances when two ro-vibrational energy levels become close for a given J value, several types of resonance interactions between these levels are possible, depending on the symmetry of states. These resonances make energy levels, wavefunctions and line intensities very sensitive to minor inaccuracies of the PES. In such cases, the computed intensity may not reflect the true accuracy of the DMS, thus a very accurate representation of the wavefunction is then needed to give a genuine transition dipole moment. This can result in huge uncertainties in the calculated intensities. To assess uncertainties of the computed intensities in the vicinity of these fragile regions, i.e. to critically evaluate or eliminate spurious results, a method of estimating the sensitivity of line intensities to theoretical model has been developed by Lodi and Tennyson [29]. This method has been successfully applied to the water molecule [29] as well to carbon dioxide [1,2], and was found to be a useful tool in finding resonances in the energetic structure of molecule, which influence the accuracy of calculated intensities. Unstable lines are often subject to intensity stealing by so-called dark states through a resonance interaction.

In this paper we report room temperature line lists for six asymmetric isotopologues of CO_2 in the 0–8000 cm^{-1} spectral region. These are $^{16}O^{12}C^{18}O$ (628), $^{16}O^{12}C^{17}O$ (627), $^{16}O^{13}C^{18}O$ (638),$^{16}O^{13}C^{17}O$ (637), $^{17}O^{12}C^{18}O$ (728) and $^{17}O^{13}C^{18}O$ (738). Cut-off value for the weighted by natural abundance intensity was set to standard 10^{-30} cm/molecule and ranges of the rotational quantum number (J) for respective isotopologues were taken from the 2012 release of the HITRAN database. Line positions are calculated using the effective Hamiltonian model [19], which takes into account the latest experiments on CO_2. This resulted in accuracy of line

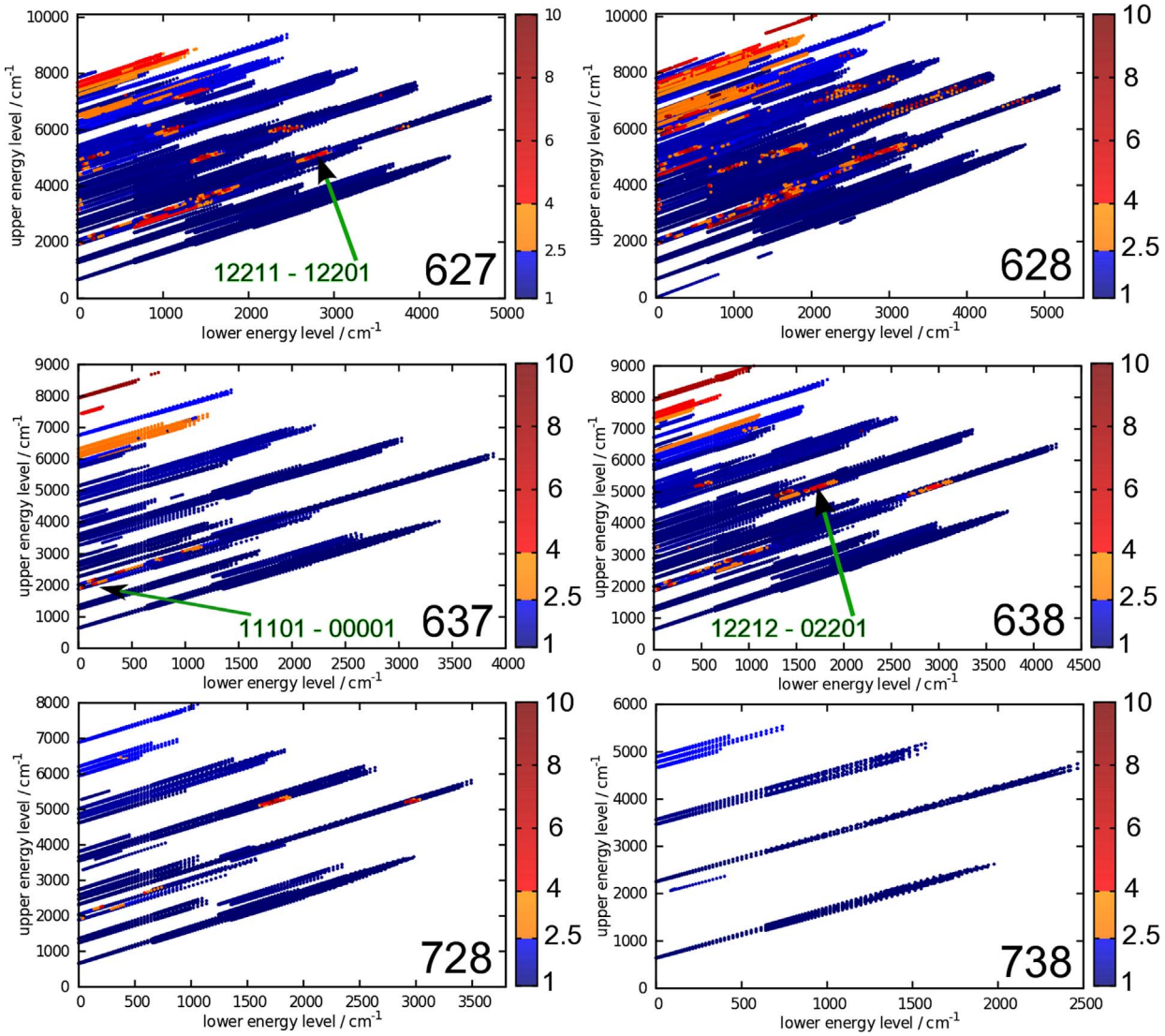

Fig. 1. Scatter factor maps for all six asymmetric isotopologues of CO_2. Colour coding classifies transitions as: stable(blue), intermediate(orange) and red(unstable). The arrows indicate examples of bands involved in resonance interactions. (For interpretation of the references to color in this figure legend, the reader is referred to the web version of this article.)

Please cite this article as: Zak EJ, et al. Room temperature linelists for CO_2 asymmetric isotopologues with *ab initio* computed intensities. J Quant Spectrosc Radiat Transfer (2017), http://dx.doi.org/10.1016/j.jqsrt.2017.01.037

positions of 0.001 cm^{-1} or better, and serves as an update to the CDSD-296 database [19] which is the most accurate and complete release available. Reducing the symmetry of CO_2 by asymmetric isotopic substitution introduces both extra allowed transitions and some extra complications in the variational nuclear motion calculations. These are discussed in the next section. Theoretical error analysis performed in Section 3.2 renders selected line intensities as reliable from the point of view of the variational method.

2. Methodology

A summary of potential energy surfaces and dipole moment surfaces used in the present work is given in Refs. [1,3,22]. In particular, our DMS ('U' below) has been demonstrated to give results of comparable accuracy to the state-of-the-art experiments [3]. In brief, we compute four independent line lists for each isotopologue, by utilizing pairs of PESs and DMSs. The first PES denoted as (Ames-1 or 'A') is a high-quality semi-empirical function published by Huang et al. [22]. The second PES denoted as (Fitted or 'F') is also a semi-empirical surface, generated by fitting an *ab initio* potential to experimental energy levels for $J = 0 - 2$ [1]. Together with our *ab initio* DMS (denoted as 'U') [3], we use the N-2 DMS from Huang et al. [22] (denoted as 'A'). This gives a set of four possible combinations of input functions used in solving the nuclear motion problem: AA, AU, FA, FU. Here the first letter stands for type of PES used and the second letter names the DMS. The line lists are then cross-matched line-by-line to yield four different values of transition intensity for each line. The ratio of the maximum to minimum intensity for each line defines the *scatter factor* ρ. A detailed interpretation of the scatter factor is given in our previous works [1,2,29]. In general, ρ accounts for instabilities of computed line intensity due to minor imperfections of the PES. The trustworthy line intensities should be stable under minor PES/DMS modifications, hence should feature a small scatter factor. In fact, the value of the scatter factor strongly reflects inaccuracies in the lowest quality PES in the considered set, thus if this quality is insufficiently high, some bands may gain a relatively high scatter factor, at the same time being very accurately modelled by our best PES/DMS combination('AU'). As shown previously [1,2], whenever a band is affected by resonance interactions, this is clearly visible as a peak in the scatter factor in the region of crossing of ro-vibrational energy levels. Based on the statistics of the scatter factor we established arbitrary limits on ρ for a line to be considered stable $(1.0 \le \rho < 2.5)$, intermediate $(2.5 \le \rho < 4.0)$ and unstable $(\rho \ge 4.0)$. These values are assumed to be the same for all isotopologues.

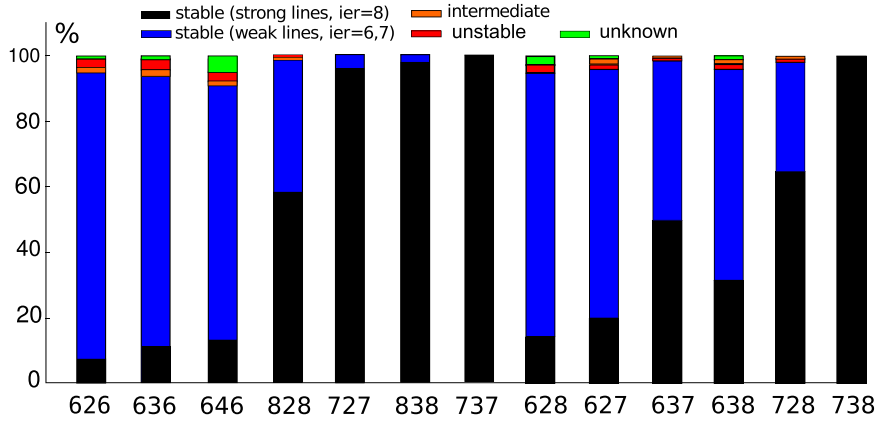

Fig. 2. Scatter factor statistics for all 13 isotopologues of carbon dioxide. Respective colours denote percentages of lines classified to particular stability domain. The *y* axis corresponds to percentage of total lines present in our line list. Black regions give percentage of stable and strong lines (>10^{-23} cm/molecule), for which the highest HITRAN intensity accuracy code was assigned (*ier*=8).

Table 2
List of selected $^{16}O^{12}C^{18}O$ vibrational bands perturbed by a resonance interaction. The columns give: vibrational quantum numbers of the perturbed band, vibrational assignment of the perturbing state, type of interaction: Inter-polyad or Coriolis, band center, total band strength, the total number of lines in the band in UCL line list, the number of stable lines, the number of intermediate lines, median of the scatter factor in the band $\tilde{\rho}$, maximum scatter factor in the band ρ_{max}, minimum scatter factor in the band ρ_{min} and instability classification: J-localized(branch) or Diffuse.

Vibrational band	Perturber	Type	Center	Strength	Total	Stable	Inter.	$\tilde{\rho}$	ρ_{max}	ρ_{min}	Stability
11111–00001	31104	Inter-pol.	4346.974	3.88E-27	154	153	1	1.2	3.1	1.1	J-local
31112–01101	51105	Inter-pol.	6263.825	1.02E-25	332	312	4	2.2	422.5	2.2	J-local
11101–00001	00011	Coriolis	2050.068	1.69E-23	277	261	9	1.2	2124.0	1.1	J-local(R)
11102–00001	00011	Coriolis	1902.447	2.95E-24	266	251	9	1.2	2599.0	1.2	J-local(R)
12212–00001	23301	Coriolis	4838.085	1.52E-26	148	138	0	1.5	15.2	1.4	J-local
23301–00001	12212	Coriolis	4825.853	1.46E-27	61	24	15	1.1	8.0	1.1	Diffuse
21112–01101	41105	Inter-pol.	4894.770	9.37E-24	448	422	2	1.5	7843.0	1.4	J-local
21102–00001	10012	Coriolis	3281.717	3.76E-25	239	138	0	1.2	115.2	1.2	Diffuse
21111–01101	41104	Inter-pol.	5063.241	2.92E-24	410	363	0	1.4	3.1×10^5	1.4	Diffuse
40014–00001	60007	Inter-pol.	7338.180	2.95E-26	134	0	123	3.6	3480.0	3.6	J-local
31113–01101	42202	Coriolis	6098.911	1.56E-25	345	326	0	2.3	7.6×10^5	2.2	Diffuse
22212–22202	25501	Cor.+l-type	2262.766	3.07E-27	227	207	0	1.0	3444.0	1.0	J-local
30003–00001	14402	Anh.+l-type	3855.968	1.43E-24	162	158	0	1.2	1.1×10^7	1.2	J-local
30013–00001	50006	Inter-pol.	6127.111	2.24E-24	165	160	0	2.3	4.6×10^5	1.3	J-local
41113–01101	61106	Inter-pol.	7459.917	2.45E-27	199	5	8	4.1	114.2	1.7	Diffuse
05521–00001	33314	Inter-pol.	7851.812	3.98E-29	14	0	0	102.2	1436.0	94.5	Diffuse

Please cite this article as: Zak EJ, et al. Room temperature linelists for CO_2 asymmetric isotopologues with *ab initio* computed intensities. J Quant Spectrosc Radiat Transfer (2017), http://dx.doi.org/10.1016/j.jqsrt.2017.01.037

Table 3
Band statistics for the asymmetric isotopologues of CO_2: 628,627,637,638,728,738. Selected are the strongest bands of each isotopologue, that have high quality experimental intensities available. The strongest bands of each isotopologue are compared between Ames-1, CDSD-296 and UCL line lists and most accurate experiments. Given for each band are the band center in cm^{-1}, the total number of measured lines in the band, J(minimum), J(maximum), experimental uncertainty range[e], the total band strength in cm/molecule, symmetric relative deviation S[a] in %, root-mean square residual (rmsr)[b] of intensity in %, the polyad number[c] change, the stability of the band based on the scatter factor analysis[d], reference to experimental data.

			J	J			UCL		Ames		CDSD				
Band	Center	Total	min	max	unc.[e]	Strength	S[a]	rmsr[b]	S	rmsr	S	rmsr	ΔP^c	T.[d]	Source
628															
00011–00001	2328.373	19	4	37	3–7	9.26×10^{-20}	0.9	2.3	−1.4	2.6	0.8	2.3	3	s	[36]
01101–00001	660.902	45	1	46	4–6	1.07×10^{-20}	1.3	3.3	1.0	3.3	−1.0	3.4	1	s	[37]
01101–00001	660.902	37	43	66	5–7	5.74×10^{-22}	3.9	7.0	3.7	6.9	0.9	5.0	1	s	[38]
10011–00001	3674.396	81	0	75	4	2.24×10^{-21}	−1.3	3.0	−1.4	3.1	0.5	2.9	5	s	[11]
10011–00001	3674.396	68	0	58	3	2.72×10^{-21}	−2.4	2.7	−2.5	2.7	−0.7	1.3	5	s	[26]
10012–00001	3569.661	78	1	76	4	2.97×10^{-21}	−2.2	3.7	−2.9	4.1	−0.3	3.1	5	s	[11]
02201–01101	665.733	121	3	52	3–7	9.36×10^{-22}	2.9	7.1	2.7	7.0	1.4	6.5	1	s	[38]
11111–01101	3685.269	102	2	62	4–5	1.99×10^{-22}	−1.8	4.5	−1.8	4.5	−0.5	4.1	5	s	[11]
11111–01101	3685.269	139	1	64	3–10	2.69×10^{-22}	0.8	23.2	−1.1	3.1	−0.0	2.9	5	s	[39]
11111–01101	3685.269	265	9	31	3	7.62×10^{-23}	−1.3	1.8	−1.3	1.8	−0.1	1.3	5	s	[26]
11112–01101	3540.235	109	1	69	4–5	1.65×10^{-22}	−0.6	4.4	−1.4	4.6	−0.1	4.3	5	s	[11]
11112–01101	3540.235	150	1	61	3–10	2.53×10^{-22}	−1.0	2.9	−1.8	3.3	−0.5	2.8	5	s	[39]
11112–01101	3540.235	19	9	36	3	5.36×10^{-23}	−1.5	1.8	−2.3	2.5	−0.7	1.4	5	s	[26]
10001–01101	701.257	78	2	52	3–7	4.52×10^{-22}	−1.8	3.8	−2.3	4.1	0.1	3.1	1	s	[38]
20012–00001	4904.123	106	0	62	3–10	1.13×10^{-22}	−1.7	3.1	−1.0	2.8	−0.2	2.8	7	s	[39]
20012–00001	4904.123	3	7	9	1	4.91×10^{-24}	0.9	1.1	1.6	1.7	2.1	2.2	7	s	[27]
20012–00001	4904.123	51	1	45	3	7.50×10^{-23}	−3.2	3.3	−2.5	2.6	−1.8	1.9	7	s	[26]
20012–00001	4904.123	116	0	67	1–2	1.28×10^{-22}	−0.2	1.4	0.5	1.5	1.4	2.2	7	s	[5]
20012–00001	4904.123	117	0	67	4–6	1.23×10^{-22}	−2.2	3.7	−1.5	3.4	−0.6	3.1	7	s	[10]
10002–01101	594.837	48	2	41	5–7	2.46×10^{-22}	17.5	19.5	17.6	19.5	1.5	8.1	1	s	[38]
20013–00001	4790.523	103	0	67	3–10	4.40×10^{-23}	−0.7	2.7	−0.3	2.6	0.4	2.8	7	s	[39]
20013–00001	4790.523	60	0	43	3	3.61×10^{-23}	−1.9	2.4	−1.5	2.2	−0.9	1.8	7	s	[26]
20013–00001	4790.523	129	0	65	1–2	4.94×10^{-23}	−1.6	3.1	−1.2	3.0	−0.4	2.5	7	s	[5]
20013–00001	4790.523	114	0	63	4–5	4.77×10^{-23}	−1.9	4.2	−1.6	4.0	−0.8	3.8	7	s	[10]
20011–00001	5041.845	82	0	48	3–10	2.29×10^{-23}	−0.5	3.4	0.9	3.5	1.3	3.8	7	s	[39]
20011–00001	5041.845	40	2	57	3–5	1.18×10^{-23}	−2.6	3.3	−1.2	2.4	−0.8	2.0	7	s	[26]
20011–00001	5041.845	110	0	58	4–6	2.39×10^{-23}	−3.7	5.7	2.3	4.9	−1.7	4.6	7	s	[10]
00021–00001	4640.227	69	0	47	3–10	1.08×10^{-23}	−2.4	3.1	−1.9	2.8	−1.1	2.3	6	s	[40]
00021–00001	4640.227	94	0	62	4–10	1.12×10^{-23}	−2.0	4.6	−1.6	4.4	−0.6	4.2	6	s	[39]
00021–00001	4640.227	97	0	56	3–10	1.29×10^{-23}	−0.1	2.4	0.3	2.4	1.2	2.9	6	s	[11]
00021–00001	4640.227	119	0	62	4–10	1.43×10^{-23}	−2.5	4.9	−2.1	4.7	−1.1	4.2	6	s	[10]
11102–10002	642.338	41	4	33	5–7	4.05×10^{-23}	3.8	6.3	3.6	6.2	−3.5	6.0	1	s	[38]
20002–00001	2613.511	102	0	57	3–10	1.98×10^{-23}	−0.9	3.2	−2.6	4.0	0.1	3.3	4	s	[39]
20002–00001	2613.511	73	0	47	3	1.80×10^{-23}	−0.6	1.0	−2.3	2.5	0.2	0.8	4	s	[26]
10001–00001	1365.107	92	0	64	5	3.05×10^{-23}	1.8	3.1	−0.4	2.5	0.3	2.8	2	s	[41]
10002–00001	1260.161	99	0	62	5	2.90×10^{-23}	0.4	3.0	–	–	−0.8	3.0	2	s	[41]
11101–10001	683.566	35	8	35	5–7	2.37×10^{-23}	2.0	4.4	1.6	4.2	2.3	4.5	1	s	[38]
20003–00001	2500.024	104	0	61	3–11	1.27×10^{-23}	−1.1	3.9	−3.3	5.0	−0.7	3.2	4	s	[39]
20003–00001	2500.024	62	3	42	3	1.00×10^{-23}	−0.2	0.8	−2.3	2.4	0.5	1.3	4	s	[26]
01111–01101	2318.568	20	18	69	3–7	1.96×10^{-23}	−2.6	4.4	−4.9	6.1	−2.5	4.4	3	s	[42]
21112–01101	4898.372	146	2	53	3–10	7.66×10^{-24}	3.6	4.6	4.2	5.1	0.5	3.1	7	u	[39]
21112–01101	4898.372	46	2	35	3–23	3.38×10^{-24}	13.0	44.6	13.7	44.9	9.6	43.2	7	u	[10]
21112–01101	4898.372	127	2	49	4–11	6.52×10^{-24}	−3.2	9.2	−2.6	9.0	−6.3	10.7	7	u	[5]
20013–10002	3531.097	32	0	47	4	6.70×10^{-24}	0.0	5.1	−0.8	5.2	−1.0	5.3	5	s	[39]
20013–10002	3531.097	49	0	49	3–8	1.05×10^{-23}	1.6	2.7	0.8	2.4	0.5	2.4	5	s	[11]
11101–00001	2047.133	62	2	63	3–33	9.79×10^{-24}	1.8	6.6	11.1	18.6	1.2	4.8	3	u	[43]
11101–00001	2047.133	25	11	41	3	5.38×10^{-24}	−2.1	2.8	8.0	9.6	−3.3	3.7	3	u	[26]
20012–10002	3648.313	26	4	45	4	4.92×10^{-24}	−0.2	4.2	−0.4	4.2	−1.8	4.6	5	s	[39]
20012–10002	3648.313	37	3	46	3–11	7.19×10^{-24}	0.7	2.4	0.5	2.3	−0.9	2.4	5	s	[11]
627															
00011–00001	2345.147	7	6	30	2–4	6.24×10^{-21}	−1.0	2.7	−3.3	4.1	0.7	2.6	3	s	[36]
00011–00001	2345.147	15	58	68	5	9.09×10^{-23}	−3.2	4.2	−5.5	6.1	−1.1	2.7	3	s	[47]
00011–00001	2345.147	15	58	68	3	9.09×10^{-23}	−3.1	4.2	−5.5	6.1	−1.1	2.8	3	s	[44]
00011–00001	2345.147	23	6	68	5	8.45×10^{-21}	−0.8	3.2	−3.1	4.4	1.2	3.4	3	s	[26]
01101–00001	667.005	35	3	39	4–8	1.44×10^{-21}	0.5	3.4	0.3	3.4	−2.9	4.9	1	s	[47]
01101–00001	667.005	38	2	56	5	1.24×10^{-21}	4.5	7.5	4.3	7.4	1.4	5.4	1	s	[37]
01111–01101	2331.998	60	5	53	3	1.48×10^{-21}	−2.1	3.4	−4.4	5.1	−0.2	2.6	3	s	[47]
01111–01101	2331.998	41	9	53	5	9.37×10^{-22}	−3.0	3.8	−5.3	5.8	−1.0	2.8	3	s	[26]
10011–00001	3694.108	87	0	59	5	7.70×10^{-22}	−2.2	2.4	−2.3	2.5	−2.1	2.3	5	s	[26]
10011–00001	3694.108	95	0	80	4	5.86×10^{-22}	−1.5	3.2	−1.6	3.3	−1.2	3.3	5	s	[11]
10012–00001	3590.512	70	0	80	4	4.44×10^{-22}	−1.5	3.5	–	−1.2	3.3	5.0	3	s	[11]
02201–01101	661.326	80	4	46	5	1.48×10^{-22}	3.4	5.4	3.1	5.2	−0.2	4.2	1	s	[47]
10001–01101	709.023	61	2	37	5	7.78×10^{-23}	−2.7	4.5	−3.2	4.8	−0.2	3.5	1	s	[47]
20012–00001	4938.605	71	0	60	5	1.55×10^{-23}	−2.6	2.7	−1.9	2.1	−0.3	0.9	7	s	[26]
20012–00001	4938.605	28	12	47	1–11	9.01×10^{-24}	−0.0	23.7	0.7	23.7	2.3	23.6	7	s	[5]

Please cite this article as: Zak EJ, et al. Room temperature linelists for CO_2 asymmetric isotopologues with *ab initio* computed intensities. J Quant Spectrosc Radiat Transfer (2017), http://dx.doi.org/10.1016/j.jqsrt.2017.01.037

Table 3 (*continued*)

Band	Center	Total	J min	J max	unc.[e]	Strength	UCL S[a]	UCL rmsr[b]	Ames S	Ames rmsr	CDSD S	CDSD rmsr	ΔP[c]	T.[d]	Source
20012–00001	4938.605	134	0	73	4–6	2.39×10^{-23}	−1.6	3.4	−0.9	3.2	0.8	3.2	7	s	[10]
20012–00001	4938.605	83	0	62	2	1.54×10^{-23}	−0.2	1.9	0.4	1.9	2.1	3.0	7	s	[12]
10002–01101	604.522	43	3	35	5	4.73×10^{-23}	11.6	13.5	11.7	13.5	−0.2	6.5	1	s	[47]
11111–01101	3704.311	150	2	72	4–10	4.03×10^{-23}	−0.8	3.5	−0.8	3.6	−0.4	3.5	5	s	[11]
11112–01101	3560.198	133	1	66	4–10	3.10×10^{-23}	−0.5	3.9	−1.3	4.1	−0.5	4.0	5	s	[11]
20013–00001	4820.757	43	0	60	5	3.02×10^{-24}	−2.0	2.4	−1.7	2.2	−0.3	1.3	7	s	[26]
20013–00001	4820.757	123	0	68	4–7	7.06×10^{-24}	−0.6	2.6	−0.3	2.5	1.3	2.8	7	s	[10]
20013–00001	4820.757	38	4	47	2–13	3.86×10^{-24}	7.9	18.3	8.2	18.5	9.6	19.2	7	s	[5]
20013–00001	4820.757	80	0	55	2	5.53×10^{-24}	0.2	1.6	0.5	1.7	1.9	2.5	7	s	[12]
20011–00001	5069.677	75	0	62	5	4.01×10^{-24}	−2.9	3.1	−1.6	1.9	−0.3	1.1	7	s	[26]
20011–00001	5069.677	131	0	67	4–7	6.07×10^{-24}	−2.0	3.5	−0.7	2.9	0.7	3.0	7	s	[10]
20011–00001	5069.677	82	0	61	2	4.21×10^{-24}	3.4	3.7	4.7	4.9	6.0	6.2	7	s	[12]
21112–01101	4930.435	296	1	59	4–7	2.67×10^{-24}	0.5	4.1	1.2	5.0	2.4	4.7	7	u	[10]
00021–00001	4654.446	280	0	62	4–7	2.11×10^{-24}	–	0.8	4.3	0.1	4.2	6.0	2	s	[10]
20012–10002	3665.553	48	1	52	4	1.49×10^{-24}	−0.0	3.1	−0.2	3.1	1.0	3.2	5	s	[11]
10001–00001	1377.543	52	1	43	5	1.35×10^{-24}	1.7	4.7	−0.5	4.4	−0.3	4.3	2	s	[41]
637															
00011–00001	2270.243	18	4	43	5	1.45×10^{-22}	1.9	2.6	−0.4	1.8	−0.3	1.8	3	s	[44]
10011–00001	3607.792	55	0	62	4	7.03×10^{-24}	5.6	6.6	5.5	6.5	−0.6	3.6	5	s	[11]
10011–00001	3607.792	28	1	48	3–10	4.96×10^{-24}	4.7	7.1	4.6	7.0	−1.6	5.7	5	s	[48]
10012–00001	3506.855	56	1	61	4	2.98×10^{-24}	5.3	6.1	4.5	5.4	−0.9	3.2	5	s	[11]
10012–00001	3506.855	12	1	38	3–13	9.00×10^{-25}	6.9	10.2	6.1	9.7	0.4	7.6	5	s	[48]
11111–01101	3620.197	51	5	53	4–7	3.85×10^{-25}	6.4	8.7	6.3	8.7	0.6	5.9	5	s	[11]
20012–00001	4848.635	75	0	50	4–9	1.91×10^{-25}	5.1	7.2	5.8	7.7	−0.8	5.1	7	s	[10]
20012–00001	4848.635	65	2	47	4–10	3.63×10^{-25}	5.1	7.1	5.7	7.6	−0.9	5.0	7	s	[48]
11112–01101	3482.365	66	4	55	4–27	1.73×10^{-25}	5.0	7.0	5.6	7.4	−1.0	4.9	5	s	[11]
20011–00001	4956.342	48	1	40	10	7.97×10^{-26}	5.8	7.6	7.1	8.6	1.1	5.0	7	s	[48]
20011–00001	4956.342	69	0	47	4–9	9.89×10^{-26}	3.4	7.5	4.6	8.1	−1.2	6.8	7	s	[10]
20013–00001	4722.116	49	3	44	4–9	1.93×10^{-26}	3.9	8.5	4.1	8.6	−0.3	7.5	7	s	[10]
00031–00001	6753.152	86	0	55	10	1.01×10^{-26}	5.9	7.6	−2.2	5.3	2.0	5.1	9	s	[15]
00021–00001	4528.497	45	4	38	4–12	5.86×10^{-27}	2.5	10.3	2.9	10.4	0.7	10.3	6	s	[11]
30012–00001	6185.757	43	2	43	10	1.99×10^{-27}	−6.1	10.7	−3.8	9.6	−0.2	8.9	9	s	[15]
20013–10002	3451.176	5	15	34	4	1.42×10^{-27}	3.7	5.4	2.8	4.9	−1.6	4.4	5	s	[11]
20011–10001	3609.826	2	12	14	4	1.22×10^{-27}	7.7	7.7	7.6	7.7	2.2	2.5	5	s	[11]
30013–00001	6074.545	28	3	33	10	7.97×10^{-28}	−7.2	11.6	−5.8	10.8	−0.3	9.1	9	u	[15]
01131–01101	6715.988	80	1	39	10	5.20×10^{-28}	0.7	9.0	−7.5	11.7	−2.8	9.3	9	s	[15]
21112–01101	4820.294	2	17	23	5–8	3.20×10^{-28}	11.3	13.5	11.9	13.9	4.6	8.6	7	u	[10]
30011–00001	6320.672	31	2	40	10	2.19×10^{-28}	−19.4	21.6	−14.4	17.2	−0.4	9.5	9	s	[15]
10031–00001	8040.610	6	6	31	10	4.56×10^{-29}	–	–	−0.4	10.4	−8.2	13.3	11	s	[15]
40013–00001	7417.626	25	4	31	10	2.22×10^{-29}	−14.4	29.4	−12.0	28.3	−40.6	48.4	11	s	[17]
10032–00001	7917.301	10	27	46	10	1.78×10^{-29}	21.7	31.4	24.5	33.4	23.9	29.0	11	s	[17]
638															
10011–00001	3588.279	51	0	54	4	3.13×10^{-23}	0.1	4.4	−0.1	4.4	−1.8	4.7	5	s	[11]
10011–00001	3588.279	76	0	61	3–10	4.79×10^{-23}	1.7	2.8	1.6	2.7	−0.0	2.2	5	s	[48]
01111–01101	2249.097	63	6	68	3–10	7.07×10^{-23}	7.9	9.3	5.5	7.4	−3.3	5.9	3	s	[48]
10012–00001	3491.854	40	2	56	4	1.32×10^{-23}	2.2	4.2	1.5	3.8	−0.8	3.9	5	s	[11]
10012–00001	3491.854	82	1	60	3–21	2.74×10^{-23}	3.0	4.3	2.2	3.9	0.0	2.9	5	s	[48]
10012–10002	2242.514	30	3	51	3–10	2.97×10^{-24}	10.0	10.4	7.7	8.2	−1.1	3.0	3	s	[48]
20012–00001	4815.291	94	0	55	3–10	1.44×10^{-24}	19.0	19.1	19.7	19.7	−0.1	1.7	7	s	[48]
20012–00001	4815.291	58	2	40	4–10	9.72×10^{-25}	0.6	21.0	1.3	21.1	−19.0	28.6	7	s	[10]
20012–00001	4815.291	1	17	18	5	5.78×10^{-26}	114.4	23.8	115.3	24.0	87.0	18.1	7	s	[5]
11112–01101	3457.958	46	5	46	4	8.69×10^{-25}	3.1	7.3	2.2	7.0	0.0	6.6	5	s	[11]
11112–01101	3457.958	63	2	40	10	1.28×10^{-24}	5.9	7.2	5.0	6.5	3.0	4.9	5	s	[48]
11111–01101	3597.621	10	16	27	4–7	4.87×10^{-25}	3.0	10.4	2.9	10.4	2.0	10.3	5	s	[11]
11111–01101	3597.621	37	2	37	10	1.60×10^{-24}	8.3	9.2	8.3	9.1	7.3	8.3	5	s	[48]
10011–10001	2240.770	19	5	48	3–11	1.30×10^{-24}	12.0	12.8	9.6	10.6	0.8	4.6	3	s	[48]
20011–00001	4925.749	121	0	48	3–14	1.09×10^{-24}	31.4	106.3	32.8	107.7	8.3	86.6	2	s	[10]
02211–02201	2231.148	8	14	52	3–10	6.02×10^{-25}	16.8	18.3	14.4	16.2	5.6	9.2	3	s	[48]
20013–00001	4690.702	69	1	47	3–10	2.09×10^{-25}	19.9	20.1	20.1	20.3	−1.1	2.9	7	s	[48]
20013–00001	4690.702	12	7	27	5–17	4.63×10^{-26}	5.4	27.2	5.6	27.2	−16.4	31.7	7	s	[10]
10001–00001	1336.378	28	7	37	5	2.36×10^{-25}	−4.1	7.7	−6.4	9.2	−0.3	6.3	2	s	[41]
00021–00001	4507.263	74	1	43	11	1.85×10^{-25}	20.8	21.0	21.2	21.3	−0.3	2.7	6	s	[48]
20002–00001	2583.005	22	6	33	15	7.86×10^{-26}	9.0	17.2	7.3	16.4	−0.2	14.6	4	s	[45]
00031–00001	6727.618	135	0	74	10	6.65×10^{-26}	17.8	18.7	9.4	11.1	0.0	5.0	9	s	[15]
10002–00001	1238.299	14	8	26	5	5.78×10^{-26}	−9.5	10.7	−12.0	13.0	−0.3	4.8	2	s	[41]
11101–00001	2005.545	20	10	36	20	4.98×10^{-26}	−3.9	25.6	10.6	27.6	−1.7	25.8	3	u	[46]
21112–01101	4797.940	50	4	33	11	4.28×10^{-26}	19.3	19.7	19.8	20.2	0.3	4.1	7	u	[48]
30012–00001	6139.386	106	0	65	10	1.72×10^{-26}	6.6	11.6	9.0	13.1	−0.8	9.4	9	s	[15]
30013–00001	6025.888	108	0	61	10	1.42×10^{-26}	8.7	12.7	10.1	13.8	−0.8	9.3	9	u	[15]
01131–01101	6692.165	211	1	64	10	5.57×10^{-27}	17.0	19.4	8.7	12.6	−0.1	8.1	9	s	[15]

Please cite this article as: Zak EJ, et al. Room temperature linelists for CO_2 asymmetric isotopologues with *ab initio* computed intensities. J Quant Spectrosc Radiat Transfer (2017), http://dx.doi.org/10.1016/j.jqsrt.2017.01.037

Table 3 (*continued*)

Band	Center	Total	J min	J max	unc.[e]	Strength	UCL S[a]	UCL rmsr[b]	Ames S	Ames rmsr	CDSD S	CDSD rmsr	ΔP[c]	T.[d]	Source
30011–00001	6278.752	74	0	61	10	1.87×10^{-27}	1.5	11.5	8.2	17.0	1.1	10.9	9	s	[15]
10031–00001	8007.762	60	1	42	5–10	1.85×10^{-27}	3.4	12.1	5.4	13.0	−0.4	11.8	11	s	[13]
31113–01101	5994.504	112	1	47	10	8.80×10^{-28}	12.5	18.8	18.5	43.8	0.1	12.3	9	u	[15]
10032–00001	7910.834	63	0	62	5–10	8.49×10^{-28}	19.4	20.1	21.9	22.5	22.6	23.2	11	s	[17]
31112–01101	6145.467	86	1	47	10	8.32×10^{-28}	7.6	15.4	9.8	16.6	−0.5	13.3	9	u	[15]
30014–00001	5875.121	42	1	46	10	6.23×10^{-28}	3.9	12.5	5.1	12.9	−0.1	11.8	9	s	[15]
02231–02201	6658.965	121	2	42	10	1.93×10^{-28}	18.5	20.9	10.1	13.9	0.9	9.2	9	s	[15]
40013–00001	7350.955	42	0	52	5–10	1.72×10^{-28}	−2.7	12.4	−0.3	12.1	−24.5	27.5	11	s	[17]
31111–01101	6307.493	76	5	44	10	1.57×10^{-28}	−0.7	13.6	5.0	14.5	−1.1	13.6	9	s	[15]
11132–01101	7862.551	119	4	44	5–10	1.25×10^{-28}	24.5	26.9	26.9	29.2	29.4	30.5	11	s	[17]
10032–10002	6665.932	51	0	42	10	8.38×10^{-29}	10.2	15.1	1.5	11.2	−1.3	10.9	9	s	[15]
20022–00001	7019.329	51	1	47	5–10	8.03×10^{-29}	10.8	20.2	13.6	21.9	17.8	23.3	10	s	[17]
40012–00001	7480.795	49	2	49	5–10	7.96×10^{-29}	4.8	12.7	9.6	15.4	−14.4	17.6	11	s	[17]
40014–00001	7219.259	35	1	32	5–10	6.50×10^{-29}	10.6	13.7	12.0	14.9	−12.8	15.5	11	u	[17]
11121–00001	6446.108	47	3	46	10	6.47×10^{-29}	7.1	16.9	7.9	17.1	−1.0	15.0	9	s	[15]
10031–10001	6669.082	39	2	40	10	3.79×10^{-29}	13.2	18.7	4.0	13.8	−8.2	15.4	9	s	[15]
20021–00001	7123.107	39	2	46	5–10	2.86×10^{-29}	10.0	24.4	14.8	26.9	23.0	23.0	10	s	[17]
11122–00001	6316.706	38	2	44	10	2.78×10^{-29}	7.4	16.6	−4.3	15.3	−3.5	13.6	9	s	[15]
40013–10002	6110.334	16	4	33	10	2.39×10^{-29}	9.3	16.5	11.4	17.8	1.3	12.9	9	s	[15]
40011–00001	7651.175	13	4	30	10–30	2.36×10^{-30}	17.2	30.3	30.1	39.6	–	–	11	s	[17]
20033–10002	7832.367	13	7	28	10–30	1.48×10^{-30}	26.7	35.7	23.5	32.0	–	–	11	s	[17]
728															
10012–00001	3546.567	83	0	62	3–10	1.74×10^{-24}	10.2	11.0	9.5	10.4	−1.5	4.6	5	s	[39]
10012–00001	3546.567	227	0	62	3	1.35×10^{-24}	8.5	8.7	7.9	8.0	−3.1	3.5	5	s	[26]
10012–00001	3546.567	75	0	83	4	1.33×10^{-24}	9.2	9.5	8.5	8.8	−2.4	3.6	5	s	[11]
00011–00001	2291.385	17	37	68	3	4.15×10^{-24}	2.3	3.8	−0.0	3.0	−0.3	3.0	3	s	[26]
10011–00001	3655.831	67	0	60	3–10	1.14×10^{-24}	7.9	8.3	7.8	8.2	−3.3	4.1	5	s	[39]
10011–00001	3655.831	64	0	59	3	9.22×10^{-25}	8.8	8.9	8.8	9.8	−2.3	2.5	5	s	[26]
10011–00001	3655.831	65	1	72	4	8.15×10^{-25}	10.0	10.3	9.9	10.3	−1.0	2.9	5	s	[11]
11112–01101	3516.783	105	3	51	3–10	1.12×10^{-25}	16.1	16.5	15.3	15.7	4.6	5.8	5	s	[39]
11112–01101	3516.783	65	3	51	3	6.95×10^{-26}	10.5	10.7	9.7	9.9	−1.2	2.3	5	s	[26]
11112–01101	3516.783	122	1	68	4	8.27×10^{-26}	11.8	12.1	11.0	11.3	0.4	2.6	5	s	[11]
11111–01101	3665.648	55	3	43	3–25	5.78×10^{-26}	15.1	16.0	15.1	16.0	4.3	6.9	5	s	[39]
11111–01101	3665.648	23	9	33	3	2.70×10^{-26}	10.8	10.9	10.9	10.9	0.1	1.1	5	s	[26]
11111–01101	3665.648	96	2	65	4	7.25×10^{-26}	11.3	11.8	11.3	11.8	0.7	3.5	5	s	[11]
20012–00001	4867.609	81	2	54	3–11	4.26×10^{-26}	10.6	10.9	11.2	11.5	−0.2	2.3	7	s	[39]
20012–00001	4867.609	51	0	60	3	2.36×10^{-26}	10.6	10.7	11.3	11.3	−0.2	1.1	7	s	[26]
20012–00001	4867.609	125	0	68	4–6	5.01×10^{-26}	11.1	11.7	11.8	12.4	0.4	3.8	7	s	[10]
20013–00001	4754.845	83	0	51	3–10	2.28×10^{-26}	10.7	11.1	11.0	11.4	−1.3	3.1	7	s	[39]
20013–00001	4754.845	54	1	57	3	1.50×10^{-26}	12.0	12.0	12.3	12.3	−0.1	0.8	7	s	[26]
20013–00001	4754.845	122	0	67	4–6	2.63×10^{-26}	11.7	12.2	12.0	12.5	−0.3	3.6	7	s	[10]
20011–00001	5013.232	49	2	42	3–14	5.03×10^{-27}	5.5	7.6	6.9	8.6	−5.7	7.6	7	s	[39]
20011–00001	5013.232	56	1	47	3	4.83×10^{-27}	11.8	11.9	13.2	13.2	0.7	1.2	7	s	[26]
20011–00001	5013.232	106	0	59	4–6	7.94×10^{-27}	10.0	11.2	11.4	12.5	−1.1	5.2	7	s	[10]
21112–01101	4861.905	58	5	31	3–30	1.65×10^{-27}	9.6	11.1	10.2	11.6	−1.5	5.8	7	u	[39]
21112–01101	4861.905	157	2	51	4–8	3.10×10^{-27}	11.3	13.1	11.8	13.6	0.3	6.6	7	u	[10]
20013–10002	3509.533	35	1	60	4	3.56×10^{-27}	13.3	13.8	12.5	13.0	2.3	4.4	5	s	[11]
20012–10002	3623.717	35	1	38	4	2.69×10^{-27}	12.9	13.5	12.7	13.3	1.9	4.4	5	s	[11]
00021–00001	4621.032	103	0	60	4–6	1.38×10^{-27}	15.0	21.9	15.5	22.2	2.2	15.5	6	s	[10]
00021–00001	4621.032	84	0	52	4–5	1.13×10^{-27}	12.2	12.7	12.7	13.1	−0.5	3.3	6	s	[11]
00031–00001	6894.409	118	0	69	10	2.06×10^{-27}	15.1	16.1	6.2	8.2	−0.1	3.9	9	s	[15]
21113–01101	4709.841	141	2	53	4–6	1.65×10^{-27}	13.7	15.0	13.9	15.2	1.5	6.1	7	s	[10]
21113–01101	4709.841	14	34	49	4–6	6.01×10^{-29}	12.4	13.0	12.7	13.2	0.2	3.7	7	s	[11]
20011–10001	3662.486	24	5	50	4–6	1.30×10^{-27}	16.6	17.7	16.7	17.7	6.2	8.7	5	s	[11]
20012–10001	3511.956	29	0	50	4–6	1.04×10^{-27}	14.1	14.8	13.5	14.2	2.5	4.9	5	s	[11]
00011–10002	1073.481	39	5	41	5	1.02×10^{-27}	−11.1	12.0	−15.1	15.7	−0.2	4.4	1	s	[44]
30013–00001	6073.047	121	0	68	10	8.58×10^{-28}	2.8	16.5	3.7	9.5	1.4	5.4	9	u	[15]
21111–01101	5037.195	115	2	40	4–6	7.38×10^{-28}	9.8	11.8	11.1	13.0	−2.6	7.1	7	u	[10]
12211–02201	3645.173	10	27	42	4–6	2.85×10^{-28}	14.2	15.3	14.3	15.4	4.1	7.0	5	s	[11]
30012–00001	6207.046	101	0	68	10	2.85×10^{-28}	−0.6	6.6	2.3	6.9	0.2	4.2	9	s	[15]
12212–02201	3463.565	24	30	53	4–6	2.83×10^{-28}	11.6	13.4	12.6	14.7	0.3	4.8	5	s	[11]
30014–00001	5946.265	103	0	65	10	1.93×10^{-28}	1.3	5.9	2.5	6.2	2.7	5.2	9	s	[15]
30013–10002	4826.273	37	3	37	10	1.46×10^{-28}	15.4	33.7	12.6	18.5	−2.1	10.0	7	s	[10]
00011–10001	961.639	15	6	28	5	1.40×10^{-28}	−6.2	7.9	−10.8	11.8	−0.3	5.0	1	s	[44]
01131–01101	6855.418	141	1	67	10	1.25×10^{-28}	14.9	16.7	6.0	9.6	1.1	5.9	9	s	[15]
30003–00001	3809.903	57	1	41	4–6	1.21×10^{-28}	11.9	13.7	11.4	13.2	0.1	5.4	6	u	[11]
21102–00001	3256.129	63	6	54	4–6	1.08×10^{-28}	14.6	17.2	13.8	16.2	−0.7	5.5	5	u	[11]
21113–11102	3473.795	16	11	32	4–6	9.87×10^{-29}	11.7	13.6	10.8	12.8	0.9	7.0	5	s	[11]
30014–10002	4696.570	26	7	35	5–7	5.64×10^{-29}	11.6	14.5	11.8	14.7	−1.4	8.8	7	s	[10]
30014–10002	4696.570	3	28	30	4	4.78×10^{-30}	13.1	15.5	14.3	15.6	1.1	6.4	7	s	[11]
31113–01101	6047.520	140	1	60	10	4.78×10^{-29}	2.0	7.6	3.3	8.0	–	–	9	u	[15]

Please cite this article as: Zak EJ, et al. Room temperature linelists for CO_2 asymmetric isotopologues with *ab initio* computed intensities. J Quant Spectrosc Radiat Transfer (2017), http://dx.doi.org/10.1016/j.jqsrt.2017.01.037

Table 3 (*continued*)

Band	Center	Total	J min	J max	unc.[e]	Strength	UCL S[a]	UCL rmsr[b]	Ames S	Ames rmsr	CDSD S	CDSD rmsr	ΔP^c	T.[d]	Source
01121–00001	5255.181	32	7	35	5–7	3.54×10^{-29}	12.1	15.3	2.1	10.0	24.7	25.9	7	s	[10]
30012–10001	4860.218	14	11	24	6–8	2.75×10^{-29}	7.7	16.3	8.4	16.6	−2.6	14.5	7	s	[10]
30002–00001	3954.525	31	5	33	5–11	2.45×10^{-29}	17.3	19.8	17.3	19.8	–	–	6	s	[11]
31112–01101	6217.194	129	1	53	10	2.42×10^{-29}	−0.4	8.5	2.3	8.8	–	–	9	s	[15]
30011–00001	6391.247	86	0	51	10	2.39×10^{-29}	−2.2	6.2	4.6	7.4	–	–	9	s	[15]
738															
10011–00001	3566.725	39	2	51	4	8.24×10^{-27}	1.8	4.5	1.7	4.5	−1.7	4.5	5	s	[11]
10012–00001	3469.362	62	0	66	4	7.67×10^{-27}	2.5	3.7	1.7	3.2	−0.0	2.8	5	s	[11]
11112–01101	3441.685	81	4	49	4	6.00×10^{-28}	1.3	4.1	0.4	3.9	−0.5	3.9	5	s	[11]
20012–00001	4773.323	56	2	43	4–11	3.36×10^{-28}	−0.6	6.9	0.0	6.9	−3.2	7.5	7	s	[10]
11111–01101	3564.013	15	11	34	4	2.25×10^{-28}	6.0	8.4	6.0	8.4	2.8	6.5	5	s	[11]
20013–00001	4663.710	38	4	32	5–9	6.25×10^{-29}	2.4	11.5	2.6	11.5	1.1	11.3	7	s	[10]
20013–00001	4663.710	20	7	31	4–5	3.31×10^{-29}	1.1	6.3	1.3	6.3	−0.3	6.2	7	s	[11]
20011–00001	4887.298	20	6	29	5–17	4.22×10^{-29}	−4.5	12.7	−3.2	12.3	−8.9	14.9	7	s	[10]
00031–00001	6698.146	91	0	63	10	2.15×10^{-29}	23.5	24.5	14.9	16.4	–	–	9	s	[15]
30013–00001	5972.284	39	3	41	10	3.59×10^{-30}	10.8	16.5	12.3	17.5	–	–	9	s	[15]
30012–00001	6085.038	34	4	39	10	3.08×10^{-30}	13.0	18.3	15.5	20.1	–	–	9	s	[15]
01131–01101	6662.913	66	1	45	10	8.80×10^{-31}	15.1	18.6	6.3	12.4	–	–	9	s	[15]
10032–00001	7869.363	67	2	47	5–10	5.86×10^{-31}	31.0	33.2	33.5	35.6	–	–	11	s	[17]

[a] see Eq. (1).
[b] rmsr: root-mean square residual.
[c] The polyad number for CO_2 is defined as: $P = 2\nu_1 + \nu_2 + 3\nu_3$, where ν_1, ν_2, ν_3 are the vibrational quantum numbers of the symmetric stretching, bending and the asymmetric stretching, respectively.
[d] Type of band: Stable('s'), unstable('u').
[e] Uncertainty interval of the measurement (in %), defined as root-mean square of statistical uncertainty plus systematic uncertainty of the measurement.

2.1. Nuclear motion calculations

The strategy for solving the nuclear-motion problem employed here is analogous to the one presented in [1] and [2]. In a nutshell, the Born-Oppenheimer approximation imposes mass-independence of the PES and DMS. With this assumption the quantum calculations for ro-vibrational energy levels, wavefunctions and transition intensities have been carried out with the DVR3D suite [30] for each isotopologue separately. However the loss of symmetry in the system meant that some (re-)evaluation of the accuracy of our variational calculations were required.

All calculations were performed in Radau coordinates and a body-fixed coordinate system with the z-axis pointing along one of the C–O bonds. Due to broken permutation symmetry of identical atoms, the full ro-vibrational Hamiltonian cannot be block-factorized, as was the case for the symmetric isotopologues. This entails substantially more computational resources to obtain a good level of convergence. A two step procedure [31–33] of solving the nuclear Schrödinger equation is applied here. The first step involves solving the Coriolis-decoupled ro-vibrational motion problem for every combination of the $(J, |k|)$ quantum numbers separately, to supply a basis for the second step, where the full ro-vibrational Hamiltonian is considered. Matrix elements of the Hamiltonian are represented on a previously optimized DVR grid, associated with 30-point Gauss-Laguerre and 120-point Gauss-Legendre quadratures, for stretching and bending motion respectively. Diagonalisation of this matrix leads to ro-vibrational energy levels and wavefunctions labelled by the J-rotational quantum number and the e/f – Wang symmetries. As done by Huang et al. [22], nuclear masses in Dalton units (Da) for isotopes of carbon and oxygen were used: 11.996709 Da (^{12}C), 13.000439 Da (^{13}C), 15.990525 Da (^{16}O), 16.995245 Da (^{17}O) and 17.995275 Da (^{18}O) [34].

A number of tests of basis sets and Hamiltonian sizes were performed to ensure convergence and stability of the calculations. However, these showed that the parameters tested and used for our study on $^{12}C^{16}O_2$ (626) [1] gave good results; these parameters were adopted except that the loss of symmetry means that size of the final Hamiltonian in the first variational step (program DVR) needs to be doubled (MAX3D=2000). Difficulties in the basis set optimisation resulting from the asymmetry in the system led to convergence problems for $J > 100$. Further extension of the size of the ro-vibrational Hamiltonian causes high J jobs to exceed our computer system wall-clock limit of 72 hours. Nevertheless, line intensities for $J > 100$ computed in our 'AA' line list remain in a very good agreement with the values provided by Ames. Therefore the ro-vibrational part of the computation (program ROTLEV3b) for all J's adopted following ro-vibrational basis size: $500 \times (J + 1)$ for $J = 0 - 50$, $400 \times (J + 1)$ for $J = 51 - 99$ and $300 \times (J + 1)$ for $J > 99$. Integral transition intensity was evaluated with appropriate spin statistical weights (cf. Table 1), partition functions computed at 296 K with energy levels from Ames-1 PES and natural abundances taken from the HITRAN2012 database. Intensity cut-off was then set to 10^{-30} cm/molecule.

2.2. Line positions

The nuclear motion calculations described in the preceding section give together with the line intensities the values of the energy levels and consequently the values of the line positions. The line positions calculated with the semi-empirical PES were used to generate UCL line list. But as we have already mentioned in the Introduction, the variational line positions are accurate to 0.03–0.2 cm^{-1}. The effective Hamiltonian models provide the line positions at least one order of magnitude more accurately [28]. The effective Hamiltonian models for the carbon dioxide isotopologues used to generate CDSD-296 [28] are based on the perturbation theory and take into account in the explicit way all vibration-rotation resonance interactions (up to sixth-order perturbation theory) arising due to the approximate relations between harmonic frequencies: $\omega_1 \approx 2\omega_2$ and $\omega_3 \approx 3\omega_2$. These relations lead to a polyad structure of the vibrational energy levels. Each polyad could be labelled with the polyad pseudo quantum number $P = 2\nu_1 + \nu_2 + 3\nu_3$, where ν_1, ν_2, ν_3 are harmonic oscillators quantum numbers. The parameters of the effective Hamiltonians for each isotopologue were fitted to the observed line positions collected from the literature (see Ref. [28] and references therein). The fitted sets of the effective Hamiltonian parameters reproduce the observed line

Please cite this article as: Zak EJ, et al. Room temperature linelists for CO_2 asymmetric isotopologues with *ab initio* computed intensities. J Quant Spectrosc Radiat Transfer (2017), http://dx.doi.org/10.1016/j.jqsrt.2017.01.037

positions with residuals which are close to the experimental uncertainties (the weighted dimensionless standard deviation varies between 1 and 2 depending on an isotopologue). The very good extrapolation abilities of these effective Hamiltonians have been demonstrated many times (see, for example, Refs. [9–11,13–16,24–26]) except for a few cases of the interpolyad resonance anharmonic interactions. These interactions, due to symmetry constraints, can take place only in the asymmetric isotopologues. In the recommended UCL-IAO line list, described below, the variational line positions are substituted by EH line positions and in a few cases when the lines are affected by the interpolyad resonance interactions the variational line positions are substituted by the experimental data if such data exist. In the absence of the experimental data the variational line positions are substituted by EH line positions.

3. Results and discussion

3.1. Summary of all CO_2 line lists

Table 1 summarizes line lists computed by us for all 13 isotopologues of CO_2 from this work and our previous studies [1,2].

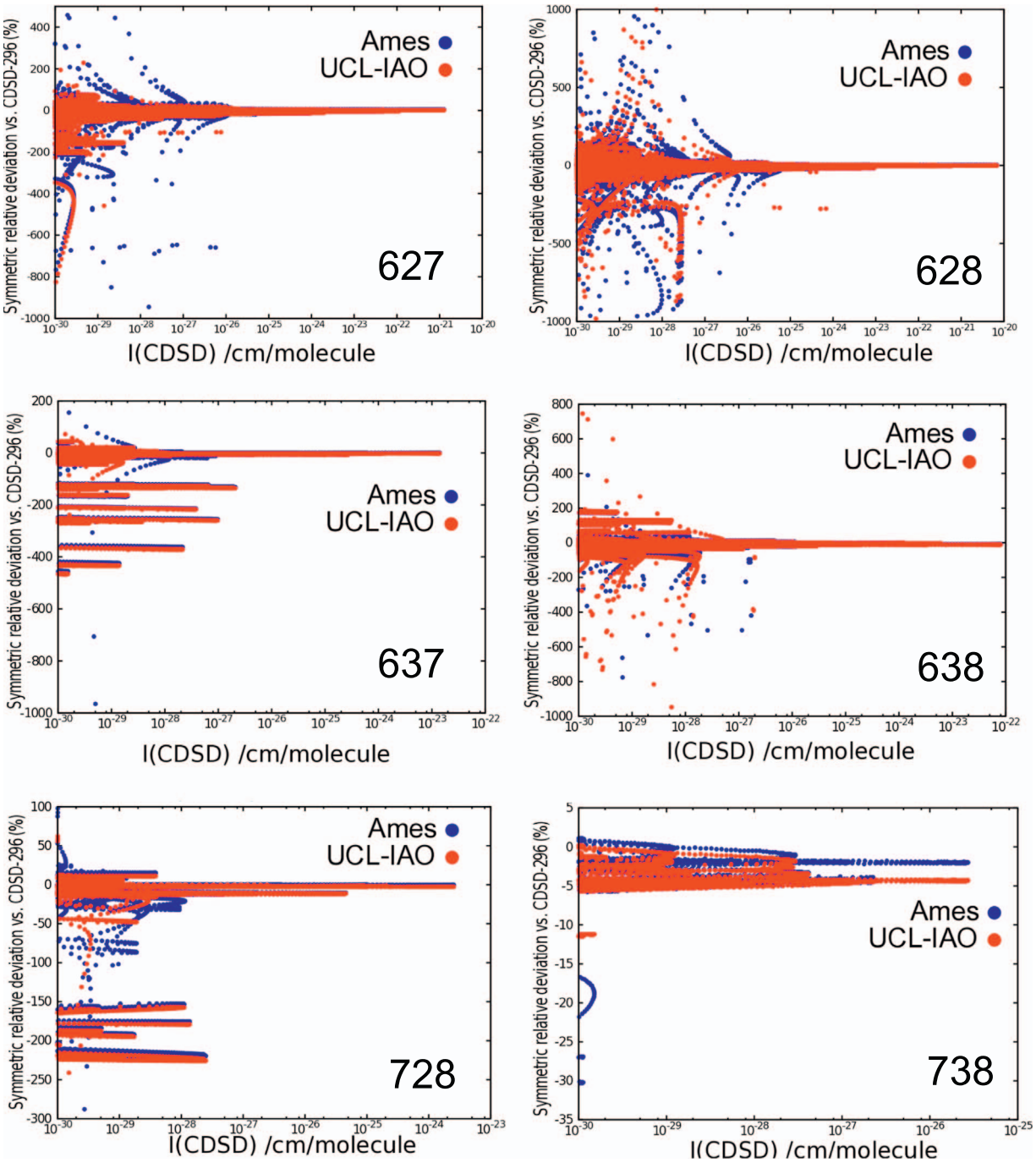

Fig. 3. Comparison of Ames and UCL line lists with the CDSD-296 database for six isotopologues of CO_2. Red and blue points denote relative percent deviation of UCL and Ames intensities from CDSD intensity, respectively. Symmetric relative deviation (see Eq. (1)) is plotted against line intensity (in cm/molecule) from CDSD-296 scaled by the natural abundance. (For interpretation of the references to color in this figure legend, the reader is referred to the web version of this article.)

Please cite this article as: Zak EJ, et al. Room temperature linelists for CO_2 asymmetric isotopologues with *ab initio* computed intensities. J Quant Spectrosc Radiat Transfer (2017), http://dx.doi.org/10.1016/j.jqsrt.2017.01.037

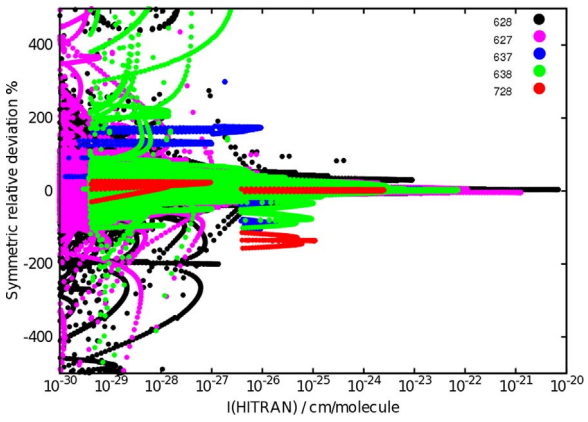

Fig. 4. General comparison of the UCL and HITRAN2012 line lists for all six asymmetric isotopologues of CO_2. Symmetric relative deviation is plotted against line intensity (in cm/molecule) from HITRAN2012 scaled by the natural abundance.

Partition functions at 296 K given in Table 1 were calculated using the DVR3D suite with the Ames-1 PES, and these are compared to the partition functions supplied by the HITRAN2012, Ames-296 and CDSD-296 line lists. The values of the partition functions computed in the present study differ from HITRAN2012 by 0.3–0.5%. This systematic shift is observed for all isotopologues, and should be taken into account in comparisons aimed at sub-percent accuracy of line intensities. On the other hand, the CDSD-296, Ames-296 and UCL line lists give values which are very close. The UCL entries are usually somewhat lower as they are computed using a smaller set of energy levels than in the original Ames-296 runs. Therefore, for line intensity calculations we used the Ames-296 partition functions from Huang et al. [22]; we recommend that room temperature CO_2 databases also adopt these values. The total numbers of lines in the HITRAN2012 database is usually lower than in remaining line lists, indicating several spectral gaps, especially for less abundant isotopologues. These gaps are all covered by our line lists. The CDSD-296 database, from which the majority HITRAN lines are taken, is heavily dependent on availability and quality of experimental data. For this reason, there are bands missing in CDSD-296, which are present in the UCL line lists. For respective isotopologues the number of these missing bands are: 159(628), 48(627), 14(637), 19(638), 2(728) and 170 (738).

3.2. Scatter factor statistics

For each isotopologue, the four computed line lists (AU, AA, FU, FA) gave rise to a scatter factor ρ of line intensities. Each transition in our primary line list (AU) received a scatter factor. Further on, vibrational bands were classified by means of this descriptor, which serves as a measure of line stability. The line list was divided into three classes of lines: stable, intermediate and unstable; following established arbitrary limits on ρ for a line to be considered stable $(1.0 \le \rho < 2.5)$, intermediate $(2.5 \le \rho < 4.0)$ and unstable $(\rho \ge 4.0)$.

Fig. 1 presents scatter factor maps introduced in our previous works. For each isotopologue, the magnitude of the scatter factor ρ for every transition is projected onto the lower energy

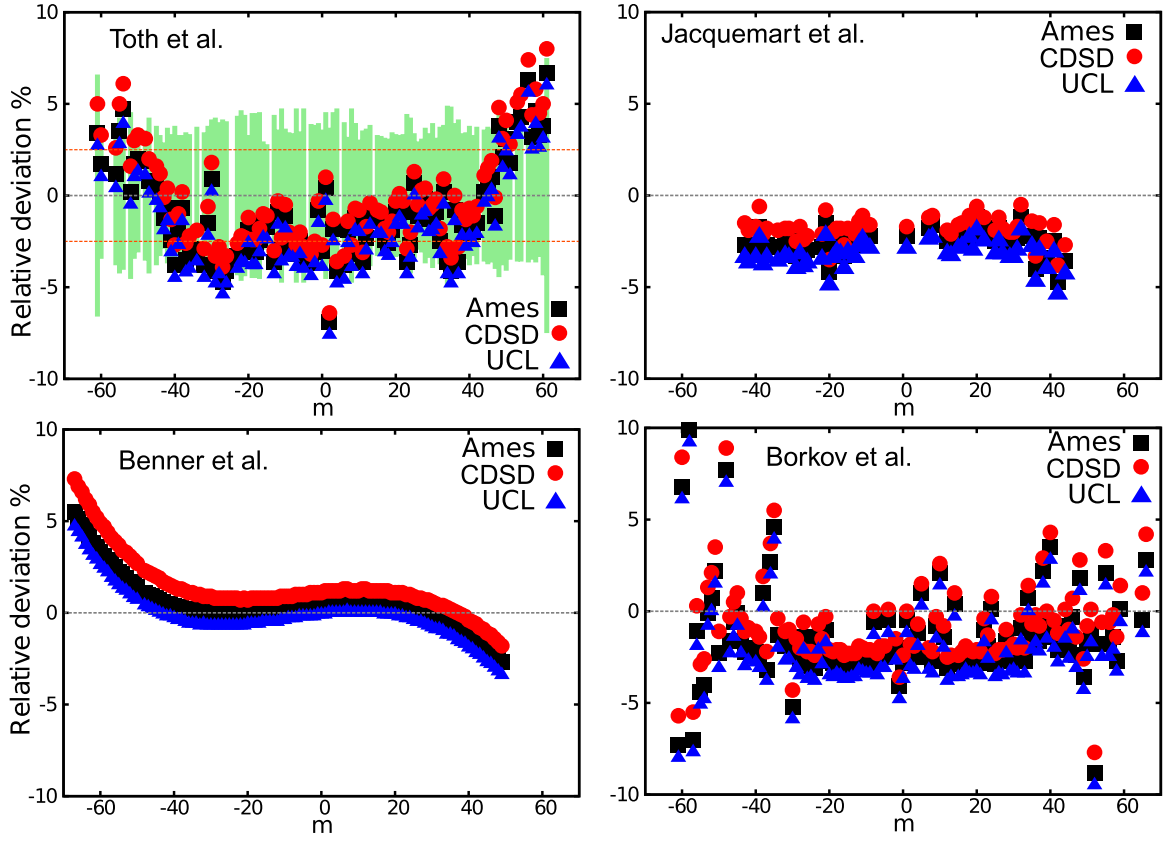

Fig. 5. Ames, CDSD-296 and UCL line intensities for the 20012–00001 band of $^{16}O^{12}C^{18}O$ compared to four recent experimental works by: Toth et al. [39] (upper left panel), Jacquemart et al. [26] (upper right panel), Benner et al. [5] (lower left panel) and Borkov et al. [10] (lower right panel). Blue triangles, red dots and black squares denote relative deviations from the measurement (in %) of UCL, CDSD-296 and Ames line intensities respectively. *m* labels rotational transitions and corresponds to *J*(lower)+1 for the R branch and -*J*(lower) for the P branch. For the left uppermost panel experimental error bars were added together with horizontal orange dashed lines indicating experimental uncertainty for the systematic shift in the transition intensity. (For interpretation of the references to color in this figure legend, the reader is referred to the web version of this article.)

Please cite this article as: Zak EJ, et al. Room temperature linelists for CO_2 asymmetric isotopologues with *ab initio* computed intensities. J Quant Spectrosc Radiat Transfer (2017), http://dx.doi.org/10.1016/j.jqsrt.2017.01.037

level – upper energy level plane. Color coding represents the value of the scatter factor, hence informs about the stability of a particular line. Few examples of unstable bands are marked with arrows in Fig. 1. Elevated values of the scatter factor correlates strongly with the presence of an interaction with an energetically proximate state. Thus, the stability analysis presented here may be utilized in extracting pairs of states, the potential candidates being involved in a mutual Coriolis or anharmonic interaction. Intensities of bands containing such states are likely to be far from experimental values, therefore we consider such bands as unreliable from the point of view of our calculations. The final recommended line lists (see Section 3.5) include line intensities for unstable bands borrowed from the empirically tuned effective dipole moment calculations or directly from measurement. Fig. 1 shows that the number of intermediate and unstable lines grows as the energy of the upper state increases. This fact is explained by the growth of the number of the energy level crossings and by deficiencies of the 'Fitted' PES, which slowly diverges from the Ames-1 PES with ;increasing energy, thus gives a poorer representation of the ro-vibrational wavefunction for high energy levels. This causes elevated values of the scatter factor, as seen in the scatter factor maps. At the same time new instability regions become visible with growing total number of transitions, i.e more abundant isotopologues have more unstable lines. For instance, the line list for the least abundant 738 isotopologue, contains no unstable lines. For 738 only very strong bands enter the line list subject to the 10^{-30} cm/molecule intensity cut-off. Strong lines are less prone to significant (percentage-wise) intensity stealing, which explains for example why the strong 00011–00001 band, resonantly interacting with the 11101 and 11102 vibrational states, remains stable. On the other hand, the relatively weak bands: 11101–00001 and 11102–00001 are strongly distorted by intensity borrowing from the 00011–00001 band. More abundant isotopologues contain more weaker bands in their spectrum, which in turn, are more likely to be unstable on account of resonance interactions. This situation is better pictured on a bar diagram given in Fig. 2, where relative percentages of stable, intermediate and unstable lines are compared among all 13 isotopologues. In general, the procedure of determining the scatter factor is very effective, leaving only sub-percent residuals of lines that could not have a scatter factor assigned. The percentages of unstable lines also oscillate around 1%, which suggests that the choice of surfaces for the line sensitivity analysis is appropriate. Experience shows that if the quality of the second (here 'Fitted') PES used in the analysis is too low, not only is it difficult to match between line lists, leading to a larger number of unknown lines, but also unnaturally high values of the scatter factor for energetically well-isolated bands arise. In such cases, a biased stability landscape, generating false positive resonances, is likely. In contrast, if this PES is too close to base PES (here the Ames-1 surface), then the spread of scatter factors could be artificially narrow, causing the unstable lines to appear to be stable. Thus the scatter factor statistics reflect the quality of the least accurate PES used rather than the uncertainty in our final results. For this reason, there is some arbitrariness in critical values adopted for the scatter factor, which categorize transitions as stable, intermediate and unstable.

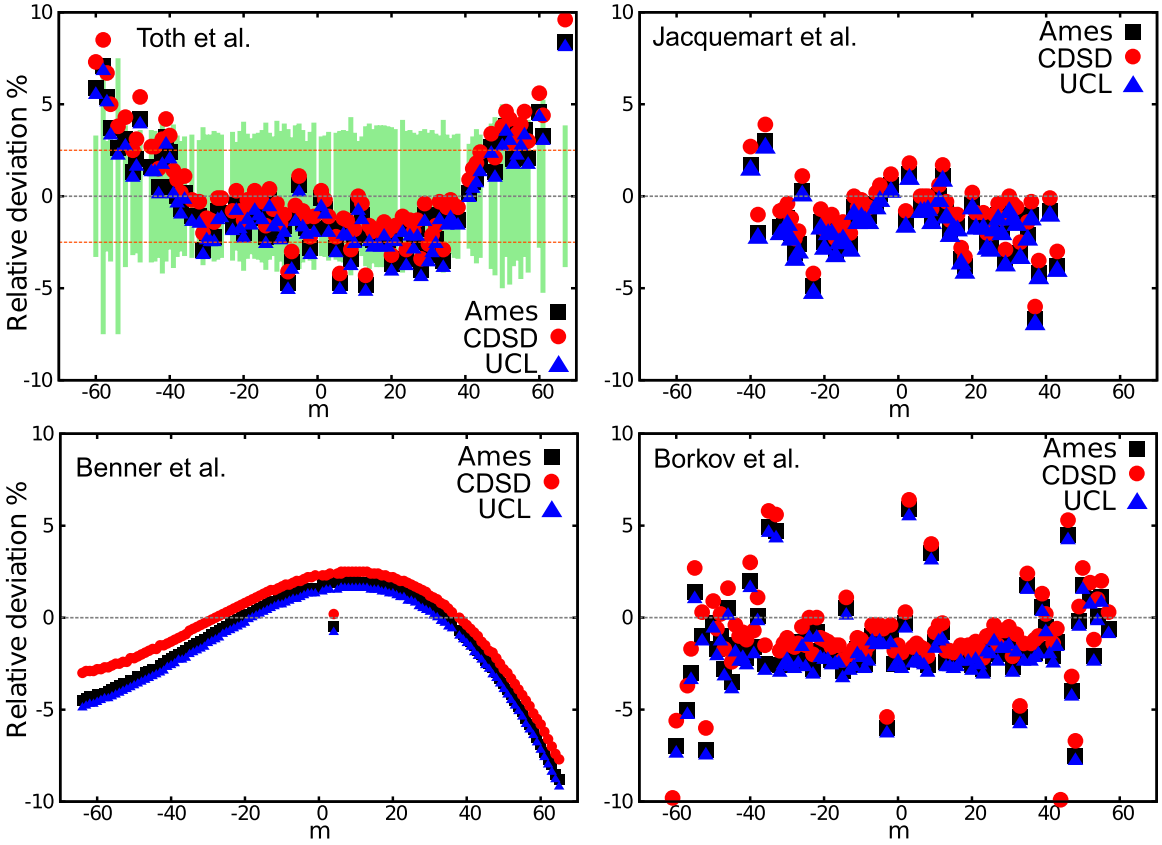

Fig. 6. Ames, CDSD-296 and UCL line intensities for the 20013 – 00001 band of $^{16}O^{12}C^{18}O$ compared to four recent experimental works by: Toth et al. [39] (upper left panel), Jacquemart et al. [26] (upper right panel), Benner et al. [5] (lower left panel) and Borkov et al. [10] (lower right panel). Blue triangles, red dots and black squares denote relative deviations from the measurement (in %) of UCL, CDSD-296 and Ames line intensities respectively. *m* labels rotational transitions and corresponds to *J*(lower)+1 for the R branch and -*J*(lower) for the P branch. For the left uppermost panel experimental error bars were added together with horizontal orange dashed lines indicating experimental uncertainty for the systematic shift in the transition intensity. (For interpretation of the references to color in this figure legend, the reader is referred to the web version of this article.)

Please cite this article as: Zak EJ, et al. Room temperature linelists for CO_2 asymmetric isotopologues with *ab initio* computed intensities. J Quant Spectrosc Radiat Transfer (2017), http://dx.doi.org/10.1016/j.jqsrt.2017.01.037

3.3. Resonances

A method of detecting lines perturbed by resonance interactions discussed in the previous sections was introduced in our previous works [1,2,29]. Table 2 gathers information about vibrational bands perturbed by a resonance interaction with other vibrational state.

Effective reproduction of experimental line intensities for 'resonance bands' is a challenge for variational calculations. Transition dipole moment being then very sensitive to small inaccuracies of the ro-vibrational wavefunction, requires almost perfect reproduction of the PES in this region, which is currently beyond reach of the variational methodology.

3.3.1. Band statistics vs. experiment

Table 3 compares measured band intensities to the calculated values from the Ames-1, UCL and CDSD-296 line lists. In general, the dipole moment surfaces of Ames and UCL appear to be of similar quality, generating band intensities that differ by few percent. A more detailed analysis reveals that both line lists follow similar intensity trends within a single band as well as between bands. The small discrepancies between Ames-1 and UCL however deserve further investigation at single line resolution followed by benchmarking against other studies. This is done in Section 3.4. For less abundant isotopologues, such as 638 and 728, deviations of theoretical line intensities from experimental values often exceed stated uncertainty of measurements [10,11,15,26], which suggests inaccuracies in retrieval procedure or in isotopic abundances in measured samples. Band intensities given by the CDSD-296 database match more closely the experimentally determined values than the remaining two line lists. The effective dipole moment calculations, on which the CDSD-296 database relies, are supplied with experimental entries, some of which have been taken from the references listed in Table 3. For this reason, CDSD-296 generates smaller overall deviations from experiment. Unfortunately, none of these measurements provide sub-percent uncertainty budget for intensities. This means one can conclude only approximately on the mutual relation between the experiments and theoretical studies (most of the measurements give 5–20% uncertainty for the line intensities). Therefore, a comparison to a preferably sub-percent accurate study is needed. One such measurement has been performed by Durry et al. [27] on three ro-vibrational lines of 628. This experiment is discussed in the following section.

Fig. 3 gives an overview of the relative agreement of the Ames and UCL line lists to CDSD-296.

For strong lines, both Ames and UCL line lists give a good overall match to CDSD-296. For weaker lines, intensity discrepancies between the line lists and CDSD become more visible, reaching several hundreds percent. Both Ames and UCL line lists follow similar pattern, which gradually diverges; the Ames line list gives a slightly larger scatter of intensities, especially for weak lines. A few bands for the 637 and 728 isotopologue are systematically shifted toward large negative deviations in intensity, hence may demand a closer attention, and perhaps a re-evaluation in the future editions of CDSD.

Fig. 4 gives an overview comparison between UCL and HITRAN2012 intensities for all six asymmetric isotopologues of CO_2. The plots use the symmetric relative deviation, S, defined by

$$S = \frac{1}{2}\left|\frac{I_{THEOR}}{I_{EXP}} - \frac{I_{EXP}}{I_{THEOR}}\right| \cdot 100\%. \quad (1)$$

The characteristic funnel-like shape is followed by the majority of lines. The 728, 637 and 638 isotopologues however, contain few moderately strong bands, exhibiting suspiciously high systematic deviations from the UCL line list. For this reason, we believe that intensities of these CDSD-296 bands cannot be trusted, and require refinement by additional experimental data or a theoretical approach. It should be noted that the majority of lines in HITRAN2012 comes from the Effective Hamiltonian calculation also enclosed in the CDSD-296 database.

3.4. Comparison to experiment

Experimental knowledge of intensities of the asymmetric isotopologues of CO_2 has been recently significantly improved by

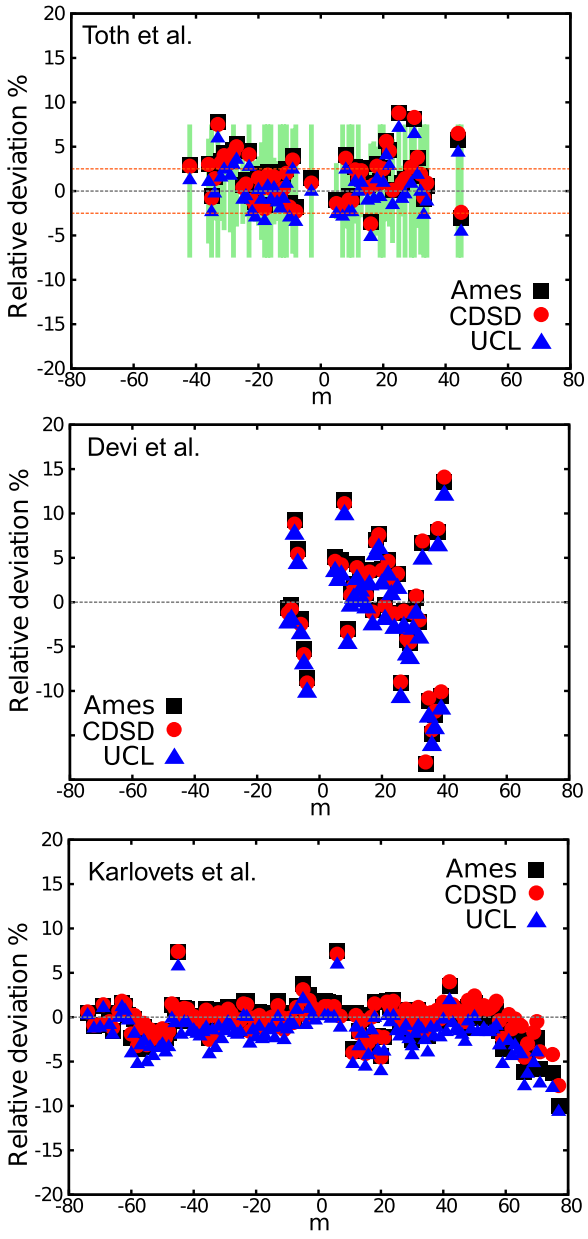

Fig. 7. Ames, CDSD-296 and UCL line intensities for the 30013–00001 band of $^{16}O^{12}C^{18}O$ compared to three recent experimental works by: Toth et al. [39] (uppermost panel), Devi et al. [4] (middle panel) and Karlovets et al. [16] (lowest panel). Blue triangles, red dots and black squares denote relative deviations from the measurement (in %) of UCL, CDSD-296 and Ames line intensities respectively. m labels rotational transitions and corresponds to J(lower)+1 for the R branch and -J(lower) for the P branch. For the uppermost panel experimental error bars were added together with horizontal orange dashed lines indicating experimental uncertainty for the systematic shift in the transition intensity. (For interpretation of the references to color in this figure legend, the reader is referred to the web version of this article.)

Please cite this article as: Zak EJ, et al. Room temperature linelists for CO_2 asymmetric isotopologues with *ab initio* computed intensities. J Quant Spectrosc Radiat Transfer (2017), http://dx.doi.org/10.1016/j.jqsrt.2017.01.037

measurements on isotopically enriched samples. This is particularly important for atmospherically relevant bands in the 1.6 μm and 2.04 μm spectral regions. Space missions [49] and ground-based observations dedicated to detection and quantification of the total carbon dioxide content in the Earth's atmosphere are based on simultaneous measurements on these two regions. Thus, due to their practical importance, the 20012–00001, 20013–00001 and 30013–00001 bands should be assessed carefully for all abundant isotopololgues, as lines from different species are likely to interfere. A line-by-line comparison with recent measurements of these three bands for the 628 isotopolgue is given below.

In Fig. 5, the four panels represent comparisons between Ames, CDSD, UCL line intensities and high-quality experiments by Toth et al. [39], Jacquemart et al. [26], Benner et al. [5] and Borkov et al. [10]. The three studies (Ames, CDSD and UCL) are denoted with black squares, red dots and blue triangles, respectively. All graphs show provisional sub-10% agreement between theory and experiment. Another common observation for all four panels is that for the 20012–00001 band line intensities are ordered as UCL < Ames < CDSD, and differences between the studies usually do not exceed 1%. This suggests similar quality of the line lists for this band. Toth et al. provides $\pm 2\%$ systematic uncertainty and J-dependent 0.5–7% statistical uncertainty on line intensities (marked with green error bars in the upper left panel of Fig. 5). UCL intensities match the stated experimental error bar, showing 2-3% systematic shift for $m \in (-30, 30)$ and characteristic, arc-like behavior for higher absolute values of m. Comparisons to Jacquemart et al. and Borkov et al. reveal small, 1–4 % systematic shift with respect to all three line lists. A markedly different situation is depicted in the left lower panel, in the study by Benner et al. Here an arc pattern of residual intensity is observed. Similar artifact has been also found in measurements on the main isotopologue of CO_2 by the same authors, and can be attributed to issue connected to the Herman-Wallis factors used in the retrieval procedure [2].

Analogous conclusions can be drawn from Fig. 6, where the UCl, CDSD and Ames line lists are compared to measurements on the 20013–00001 band. Note that all three line lists give an average negative systematic shift with respect to the experimental values. Line intensities of the 20012–00001 and 20013–00001 bands together with the line intensities of other five bands published by Toth et al. [39] were used for the determination of the concentration of the $^{16}O^{12}C^{18}O$ isotopologue in the sample used by Jacquemart et al. [26] and Borkov et al. [10]. This may indicate that the experimental studies underestimate the concentration of the 628 isotopologue, causing the intensities of individual lines to be systematically overestimated.

Intensities for the 30013–00001 band of $^{16}O^{12}C^{18}O$ (called 'the weak CO_2 band') have been accurately determined in three studies. The uppermost panel in the Fig. 7 compares UCL, CDSD and Ames line intensities for this band to measurements by Toth et al. [39]. All three theoretical studies match the experimental error bars. UCL intensities (blue triangles) provide an almost zero systematic shift for this band. The J-dependent scatter of relative deviations between theory and experiment is most likely caused by the statistical fluctuations of the experiment. A very similar picture

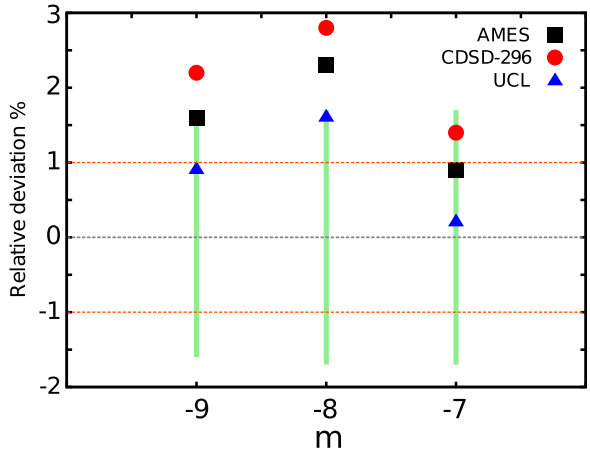

Fig. 8. Experimental line intensities measured by Durry et al. [27] for the P branch of the 20012 – 00001 band of $^{16}O^{12}C^{18}O$ depicted against respective transition intensities taken from Ames, CDSD-296 and UCL line lists. m labels rotational transitions and corresponds to J(lower)+1 for the R branch and -J(lower) for the P branch.

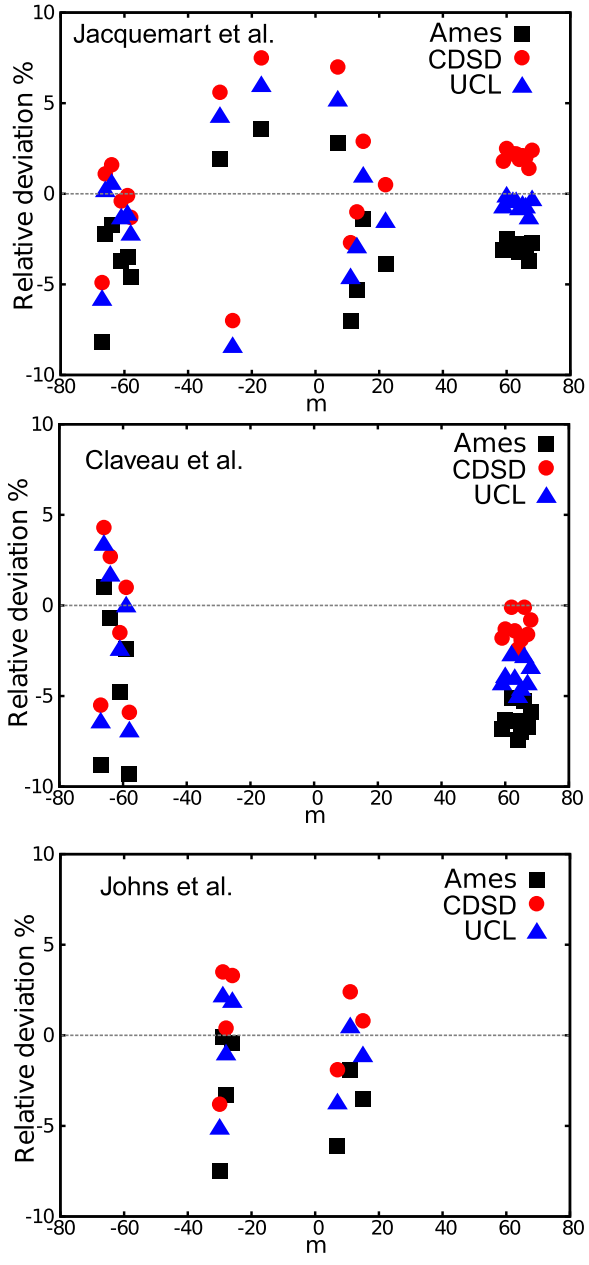

Fig. 9. Ames, CDSD-296 and UCL line intensities for the 00011–00001 band of $^{16}O^{12}C^{17}O$ compared to three experimental works by: Jacquemart et al. [26] (uppermost panel), Claveau et al. [47] (middle panel) and Johns et al. [36] (lowest panel). Blue triangles, red dots and black squares denote relative deviations from the measurement (in %) of UCL, CDSD-296 and Ames line intensities respectively. m labels rotational transitions and corresponds to J(lower)+1 for the R branch and -J(lower) for the P branch. (For interpretation of the references to color in this figure legend, the reader is referred to the web version of this article.)

Please cite this article as: Zak EJ, et al. Room temperature linelists for CO_2 asymmetric isotopologues with *ab initio* computed intensities. J Quant Spectrosc Radiat Transfer (2017), http://dx.doi.org/10.1016/j.jqsrt.2017.01.037

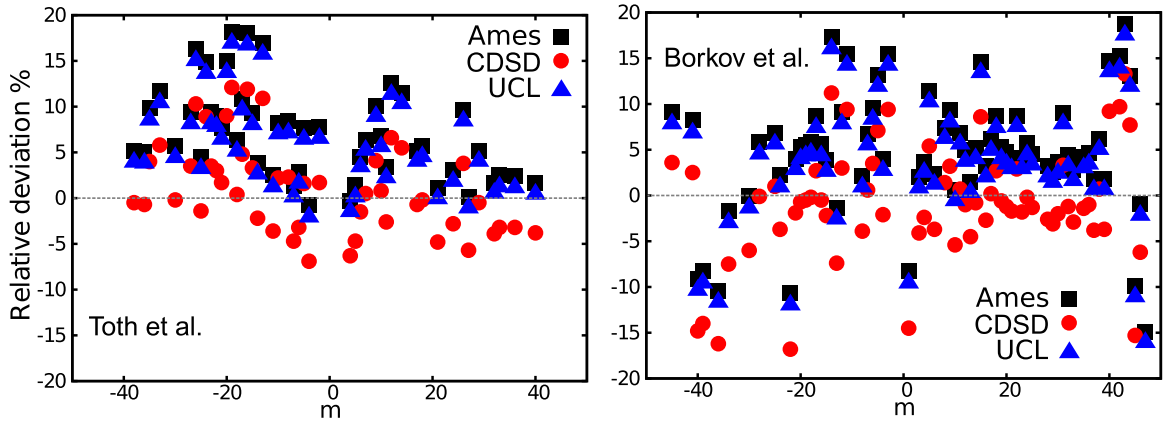

Fig. 10. Ames, CDSD-296 and UCL line intensities for the 20011–00001 band of $^{16}O^{13}C^{17}O$ compared to two experimental works by: Toth et al. [48] (left panel) and Borkov et al. [10] (right panel). Blue triangles, red dots and black squares denote relative deviations from the measurement (in %) of UCL, CDSD-296 and Ames line intensities respectively. *m* labels rotational transitions and corresponds to *J*(lower)+1 for the R branch and -*J*(lower) for the P branch. (For interpretation of the references to color in this figure legend, the reader is referred to the web version of this article.)

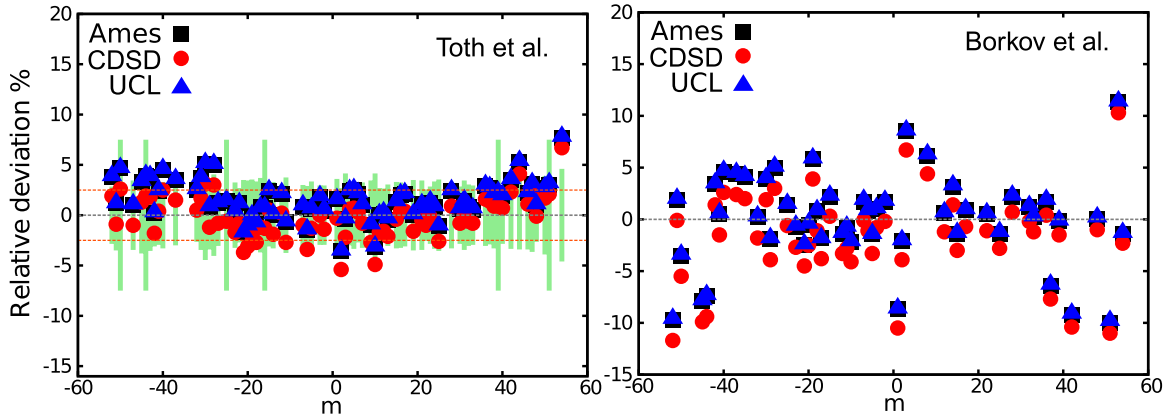

Fig. 11. Ames, CDSD-296 and UCL line intensities for the 10011–00001 band of $^{16}O^{13}C^{18}O$ compared to two experimental works by: Toth et al. [48] (left panel) and Borkov et al. [11] (right panel). Blue triangles, red dots and black squares denote relative deviations from the measurement (in %) of UCL, CDSD-296 and Ames line intensities respectively. *m* labels rotational transitions and corresponds to *J*(lower)+1 for the R branch and -*J*(lower) for the P branch. In the left panel experimental error bars were added together with horizontal orange dashed lines indicating experimental uncertainty for the systematic shift in the transition intensity. (For interpretation of the references to color in this figure legend, the reader is referred to the web version of this article.)

emerges from the middle graph in Fig. 7. Here the experimental scatter (Devi et al.) reaches 20%, whereas the systematic shift is again close to 0%. One possible explanation for this is a lower signal-to-noise ratio in the experiment of Devi et al., although inconsistent retrievals from crude data could be also the cause. The lowest panel in Fig. 7 depicts measurements by Karlovets et al. on ^{18}O-enriched samples. Except for two points with large discrepancies at $m=-44$ and $m=+8$, the comparison gives an overall very good agreement with Ames, CDSD and UCL, with average systematic shift of 1–2%. The 30013–00001 band has been previously verified to be reproduced at sub-percent accuracy for the main 626 isotpologue [1], and less abundant symmetric 636 isotopologue [6]. Results shown and discussed above support the thesis, that our DMS is capable of reproducing the true line intensities in the 1.6 μm region with accuracy not worse than 1–3% for the asymmetric isotopologues and 1% or better for the symmetric ones. For the 2.06 μm region, containing the 'the strong CO_2 bands' a thorough investigation of line intensities was made in our previous papers, concluding that sub-percent accuracy is given by the UCL calculated intensities for the 20013–00001 and 20012–00001 bands. The essential question to ask is, whether this high accuracy is transferable to the asymmetric isotopologues.

Durry et al. [27] performed intensity measurements with a near-infrared tunable diode laser spectrometer providing 1% stated accuracy and sub-percent precision on a sample containing $^{16}O^{12}C^{18}O$ in the 2.06 μm spectral region. Results of this experiment are compared to the Ames, CDSD-296 and UCL line intensities in Fig. 8. To the best of our knowledge, this is the most accurate intensity measurement reported on an asymmetric isotopologue of carbon dioxide. From the Fig. 8 it is readily seen that only the UCL line intensities for P(7), P(8) and P(9) lines match the experimental error bar. An average systematic shift of +1% is observed for the UCL intensities, +1.5% for Ames and +2.0% for CDSD-296. Thus, we tentatively conclude on plausible sub-percent accuracy of UCL line intensities for this band.

Fig. 9 compares transition intensities from different measurements for the asymmetric stretching fundamental (00011–00001 band) of the 627 isotopologue. Experiments by Jacquemart et al. [26] (uppermost panel in Fig. 9), Claveau et al. [47] (middle panel in Fig. 9) have stated 5% systematic uncertainty and undetermined statistical uncertainty, while measurements by Johns et al. [36] (lowest panel in Fig. 9) have 2% stated systematic uncertainty and 2–3% statistical uncertainty. Ames, CDSD and UCL line lists give similar deviations from experiments, showing systematic shifts smaller than 5%. For all three panels in Fig. 9, Ames transition intensities are usually weaker than UCL intensities, whereas CDSD intensities are usually stronger than UCL intensities. At the same time UCL lines give the smallest systematic deviation from experiments.

Please cite this article as: Zak EJ, et al. Room temperature linelists for CO_2 asymmetric isotopologues with *ab initio* computed intensities. J Quant Spectrosc Radiat Transfer (2017), http://dx.doi.org/10.1016/j.jqsrt.2017.01.037

Fig. 10 displays comparison between two experimental studies by Toth et al. [48] (left panel) and Borkov et al. [10] (right panel) respectively, and three line lists: Ames, CDSD and UCL. The former experiment has stated 2.5% systematic uncertainty and 10% statistical uncertainty, while the latter experiment has 4% systematic uncertainty and 0.5–7% statistical uncertainty. The agreement between measurements and line lists reflects the relatively high uncertainties, showing similar statistical scatter for all three line lists, but essentially smaller systematic deviation for the CDSD line list, which was constructed by fitting to measurements by Toth et al. Systematic deviation from experiment is again very similar (around 1%) for UCL and Ames intensities. Also, CDSD, Ames and UCL follow the same pattern, indicating that the statistical scatter visible in Fig. 10 is of experimental origin.

In Fig. 11, which compares Ames, CDSD and UCL line lists to experiments by Toth et al. [48] (left panel) and Borkov et al. [11] (right panel), large deviations of Ames and UCL from measured line intensities are visible for several lines of the P branch of the 10011–00001 band in $^{16}O^{13}C^{18}O$. The Ames and UCL line lists provide similar values of transition intensities for these lines (agreement within 2%), whereas CDSD intensities do not exhibit any unusual deviation. This observation can be rationalized by the fact that effective operators used to construct the CDSD database were parametrized by experimental intensities from Ref. [48]. The statistical scatter of the measured line intensities indicates insufficient experimental precision. Average systematic shift from measurements is within 1% for the CDSD, Ames and UCL line lists.

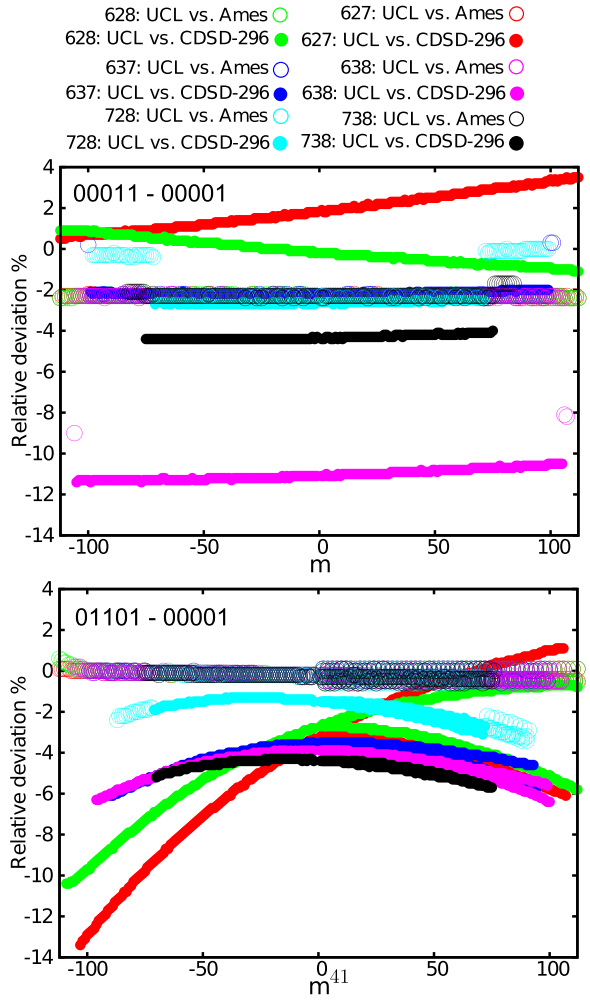

Fig. 12. Comparison of intensities of two fundamental bands for all six asymmetric isotopologues of CO_2, between UCL, Ames and CDSD line lists. *m* labels rotational transitions and corresponds to *J*(lower)+1 for the R branch and -*J*(lower) for the P branch.

Another problem to address is how intensities of lines transfer between isotopologues for the Ames and UCL line lists, and how do they relate to CDSD-296. It is eye-catching in Fig. 12 that Ames and UCL intensities for the 00011–00001 and 01101–00001 bands are very similar, showing agreement at <0.5% level for the majority of lines. In contrast, line intensities from CDSD give significant systematic shifts and noticeable arc structures, characteristic for the empirically determined quantities. Therefore, we may expect Ames and UCL to exhibit similar behavior with isotopic substitution. Here, no discontinuity in intensity pattern around $J=0$ is observed for the Ames line lists, unlike for the main isotopologue [23].

3.5. Recommended line lists

For all six asymmetric isotopologues two types of line lists were prepared. First, files named 'UCL-296-isotopologue_ name.dat' contain line positions calculated using Ames-1 PES with DVR3D program and line intensities using UCL DMS ('AU' line list). Each line is supplemented with the appropriate scatter factor ρ, given in the last column. Vibrational assignments are taken from the newest version of the CDSD-296 database. The second type of line lists, denoted "recommended-UCL-IAO-296-isotopologue_ name.dat" borrows line positions from the effective Hamiltonian calculations (see Section 2.2), and in the sporadic cases of the lines affected by the interpolyad anharmonic resonance interactions, from experimental data. Appropriate sources of experimental data used are given in the Supplementary materials.

Intensities of stable lines belonging to bands stronger than 10^{-23} cm/molecule (for unit abundance) were taken from UCL DMS calculations and assigned HITRAN uncertainty code 8 (i.e. accuracy of 1% or better). Stable lines belonging to parallel bands weaker than 10^{-23} cm/molecule also come from UCL DMS computation and were given uncertainty code 7 (i.e. accuracy 1–2 %). Intermediate lines and stable lines belonging to perpendicular bands weaker than 10^{-23} cm/molecule feature HITRAN uncertainty code 6 (i.e. accuracy 2–5%). Line intensities of bands containing $3\nu_3$ vibrational excitation as well as unstable lines were taken from the effective Hamiltonian calculations.

All line positions and line intensities for which a scatter factor was not assigned were taken from the effective Hamiltonian computation. This was the case for a total of only 975 weak lines summing over all isotopologues. Both types of line lists are given in the supplementary materials with suitable explanation in the text files. Abundances for each isotopologue were taken from the HITRAN2012 database and the final line lists used an abundance-scaled intensity cut-off 10^{-30} cm/molecule.

4. Summary

In the present study we compute new line lists for six asymmetric isotopologues of carbon dioxide: $^{16}O^{12}C^{18}O$, $^{16}O^{12}C^{17}O$, $^{16}O^{13}C^{18}O$, $^{16}O^{13}C^{17}O$, $^{17}O^{12}C^{18}O$ and $^{17}O^{13}C^{18}O$. A mixed *ab initio* -empirical methodology used to produce the line lists provide complete spectral coverage up to 8000 cm^{-1}, with line positions generated using an effective Hamiltonian model, supporting accuracy reaching the resolution of a typical FT-IR spectroscopic measurement and reliable intensities given at sub-percent accuracy for selected strong bands and 2–5% accuracy for the rest of lines. This is confirmed by detailed comparisons to the HITRAN2012, CDSD-296 and Ames-1 line lists, as well as to recent high-quality experiments on isotopically enriched samples of carbon dioxide. A method of varied input potential surfaces and

dipole moment surfaces is presented here as a useful tool in the search of energy levels perturbed by vibration-rotation resonance interactions including interpolyad-type resonances. This sensitivity analysis of the line intensities validates the majority of computed line intensities as reliable, which means that nearly all entries in our line lists can be given an uncertainty based on purely theoretical considerations. We hope that the methodology presented and evaluated here will be of use in theoretical approaches to other molecules. Line lists reported in the present paper, together with line profile parameters from other works [50], are recommended for use in remote sensing studies and inclusions in databases. This paper completes our analysis of the transition intensities of all 12 stable isotopologues of CO_2 plus the radioactive $^{14}C^{16}O_2$ isotopologue up to 8000 cm^{-1} [1,2]. It would be clearly useful to extend this work to higher wavenumbers but that requires further work on the DMS to ensure appropriate accuracy of these shorter wavelength transitions.

Acknowledgments

This work is supported by the UK Natural Environment Research Council (NERC) through Grant NE/J010316, the ERC under the Advanced Investigator Project 267219 and the Russian Fund for Fundamental Science. The authors acknowledge the use of the UCL Legion High Performance Computing Facility (Legion@UCL), and associated support services, in the completion of this work.

Appendix A. Supplementary data

Supplementary data associated with this article can be found in the online version at http://dx.doi.org/10.1016/j.jqsrt.2017.01.037.

References

[1] Zak E, Tennyson J, Polyansky OL, Lodi L, Tashkun SA, Perevalov VI. A room temperature CO_2 line list with ab initio computed intensities. J Quant Spectrosc Radiat Transf 2016;177:31–42. http://dx.doi.org/10.1016/j.jqsrt.2015.12.022.

[2] Zak EJ, Tennyson J, Polyansky OL, Lodi L, Tashkun SA, Perevalov VI. Room temperature line lists for CO_2 symmetric isotopologues with ab initio computed intensities. J Quant Spectrosc Radiat Transf 2017;189:267–280. http://dx.doi.org/10.1016/j.jqsrt.2016.11.022.

[3] Polyansky OL, Bielska K, Ghysels M, Lodi L, Zobov NF, Hodges JT, et al. High accuracy CO_2 line intensities determined from theory and experiment. Phys Rev Lett 2015;114:243001. http://dx.doi.org/10.1103/PhysRevLett.114.243001.

[4] Devi VM, Benner DC, Sung K, Brown LR, Crawford TJ, Miller CE, et al. Line parameters including temperature dependences of self- and air-broadened line shapes of $^{12}C\ ^{16}O_2$: 1.6-μm region. J Quant Spectrosc Radiat Transf 2016;177:117–144. http://dx.doi.org/10.1016/j.jqsrt.2015.12.020.

[5] Benner DC, Devi VM, Sung K, Brown LR, Miller CE, Payne VH, et al. Line parameters including temperature dependences of air- and self-broadened line shapes of $^{12}C^{16}O_2$:2.06-μm region. J Mol Spectrosc 2016;326:21–47. http://dx.doi.org/10.1016/j.jms.2016.02.012.

[6] Kiseleva M, Mandon J, Persijn S, Petersen J, Nielsen L, Harren FJM. Tractable line strength measurements of methane and carbon dioxide in the near infrared wavelength region at 1.65 μm using cavity ring down spectroscopy. In: Proceedings of the 13th ASA-HITRAN conference. Reims; 2016. p. P1–6.

[7] Brunzendorf J, Werwein V, Serduykov A, Werhahn O, Ebert V. CO_2 line strength measurements in the 20012–00001 band near 2 μm. In: The 24th colloquium on high resolution molecular spectroscopy; 2015. p. O17.

[8] Shved GM. On the abundances of carbon dioxide isotopologues in the atmospheres of mars and earth. Sol Syst Res 2016;50:161–164. http://dx.doi.org/10.1134/S0038094616020064.

[9] Jacquemart D, Borkov Y, Lyulin OM, Tashkun SA, Perevalov VI. Fourier transform spectroscopy of CO_2 isotopologues at 1.6 μm: line positions and intensities. J Quant Spectrosc Radiat Transf 2015;160:1–9. http://dx.doi.org/10.1016/j.jqsrt.2015.03.016.

[10] Borkov YG, Jacquemart D, Lyulin OM, Tashkun SA, Perevalov VI. Infrared spectroscopy of ^{17}O- and ^{18}O-enriched carbon dioxide: line positions and intensities in the 4681–5337 cm^{-1} region. J Quant Spectrosc Radiat Transf 2015;159:1–10. http://dx.doi.org/10.1016/j.jqsrt.2015.02.019.

[11] Borkov YG, Jacquemart D, Lyulin OM, Tashkun SA, Perevalov VI. Infrared spectroscopy of ^{17}O- and ^{18}O-enriched carbon dioxide: line positions and intensities in the 3200–4700 cm^{-1} region. Global modeling of the line positions of $^{16}O^{12}C^{17}O_2$ and $^{17}O^{12}C^{17}O$. J Quant Spectrosc Radiat Transf 2014;137:57–76. http://dx.doi.org/10.1016/j.jqsrt.2013.11.008.

[12] Jacquemart D. Private communication; 2014.

[13] Karlovets EV, Kassi S, Tashkun SA, Perevalov VI, Campargue A. High sensitivity cavity ring down spectroscopy of carbon dioxide in the 1.19–1.26 μm region. J Quant Spectrosc Radiat Transf 2014;144:137–153. http://dx.doi.org/10.1016/j.jqsrt.2014.04.001.

[14] Karlovets EV, Campargue A, Mondelain D, Béguier S, Kassi S, Tashkun SA, et al. High sensitivity cavity ring down spectroscopy of ^{18}O enriched carbon dioxide between 5850 and 7000 cm^{-1}: I. Analysis and theoretical modeling of the $^{16}o^{12}c^{18}$ spectrum. J Quant Spectrosc Radiat Transf 2013;130:116–133. http://dx.doi.org/10.1016/j.jqsrt.2013.05.019.

[15] Karlovets EV, Campargue A, Mondelain D, Kassi S, Tashkun SA, Perevalov VI. High sensitivity Cavity Ring Down spectroscopy of ^{18}O enriched carbon dioxide between 5850 and 7000 cm^{-1}: Part III Analysis and theoretical modeling of the $^{12}C^{17}O_2$, $^{16}O^{12}C^{17}O$, $^{17}O^{12}C^{18}O$, $^{16}O^{13}C^{17}O$ and $^{17}O^{13}C^{18}O$ spectra. J Quant Spectrosc Radiat Transf 2014;136:89–107. http://dx.doi.org/10.1016/j.jqsrt.2013.11.006.

[16] Karlovets E, Campargue A, Mondelain D, Kassi S, Tashkun S, Perevalov V. High sensitivity Cavity Ring Down spectroscopy of ^{18}O enriched carbon dioxide between 5850 and 7000 cm^{-1}: Part III Analysis and theoretical modeling of the $^{12}C^{18}O_2$, $^{13}C^{18}O_2$ and $^{16}O^{13}C^{18}O$ spectra. J Quant Spectrosc Radiat Transf 2014;136:71–88. http://dx.doi.org/10.1016/j.jqsrt.2013.11.005.

[17] Kassi S, Karlovets E, Tashkun S, Perevalov V, Campargue A. Analysis and theoretical modeling of the 18O enriched carbon dioxide spectrum by CRDS near 1.35 μm: (i) $^{16}O^{12}C^{18}O$, $^{16}O^{12}C^{17}O$, $^{16}O^{12}C^{16}O$ and $^{16}O^{13}C^{16}O$. J Quant Spectrosc Radiat Transf 2017;187:414–425. http://dx.doi.org/10.1016/j.jqsrt.2016.09.002.

[18] Rothman LS, Gordon IE, Babikov Y, Barbe A, Benner DC, Bernath PF, et al. The HITRAN 2012 molecular spectroscopic database. J Quant Spectrosc Radiat Transf 2013;130:4–50. http://dx.doi.org/10.1016/jqsrt.2013.07.002.

[19] Tashkun SA, Perevalov VI, Gamache RR, Lamouroux J. CDSD-296, high resolution carbon dioxide spectroscopic databank: version for atmospheric applications. J Quant Spectrosc Radiat Transf 2015;152:45–73. http://dx.doi.org/10.1016/j.jqsrt.2014.10.017.

[20] Jacquinet-Husson N, Armante R, Scott NA, Chédin A, Crépeau L, Boutammine C, et al. The 2015 edition of the GEISA spectroscopic database. J Mol Spectrosc 2016;327:31–72. http://dx.doi.org/10.1016/j.jms.2016.06.007.

[21] Miller CE, Crisp D, DeCola PL, Olsen SC, Randerson JT, Michalak AM, et al. Precision requirements for space-based X-CO2 data. J Geophys Res 2007;112:D10314. http://dx.doi.org/10.1029/2006JD007659.

[22] Huang X, Schwenke DW, Tashkun SA, Lee TJ. An isotopic-independent highly accurate potential energy surface for CO_2 isotopologues and an initial $^{12}C^{16}O_2$ infrared line list. J Chem Phys 2012;136:124311. http://dx.doi.org/10.1063/1.3697540.

[23] Huang X, Gamache RR, Freedman RS, Schwenke DW, Lee TJ. Reliable infrared line lists for 13 CO_2 isotopologues up to E=18,000 cm^{-1} and 1500 K, with line shape parameters. J Quant Spectrosc Radiat Transf 2014;147:134–144. http://dx.doi.org/10.1016/j.jqsrt.2014.05.015.

[24] Tan Y, Zhao X-Q, Liu A-W, Hu S-M, Lyulin OM, Tashkun SA, et al. Cavity ring-down spectroscopy of CO_2 overtone bands near 830 nm. J Quant Spectrosc Radiat Transf 2015;165:22–27. http://dx.doi.org/10.1016/j.jqsrt.2015.06.010.

[25] Vasilchenko S, Konefal M, Mondelain D, Kassi S, Čermák P, Tashkun SA. The CO2 absorption spectrum in the 2.3 μm transparency window by high sensitivity CRDS: (i) rovibrational lines. J Quant Spectrosc Radiat Transf 2016;184:233–240. http://dx.doi.org/10.1016/j.jqsrt.2016.07.002.

[26] Jacquemart D, Gueye F, Lyulin OM, Karlovets EV, Baron D, Perevalov VI. Infrared spectroscopy of CO_2 isotopologues from 2200 to 7000 cm^{-1}: I—Characterizing experimental uncertainties of positions and intensities. J Quant Spectrosc Radiat Transf 2012;113:961–975. http://dx.doi.org/10.1016/j.jqsrt.2012.02.020.

[27] Durry G, Li JS, Vinogradov I, Titov A, Joly L, Cousin J, et al. Near infrared diode laser spectroscopy of C_2H_2, H_2O, CO_2 and their isotopologues and the application to TDLAS, a tunable diode laser spectrometer for the martian PHOBOS-GRUNT space mission. Appl Phys B 2010;99:339–351. http://dx.doi.org/10.1007/s00340-010-3924-y.

[28] V.I.PerevalovS.A.TashkunCDSD-296 (Carbon Dioxide Spectroscopic Databank): updated and enlarged version for atmospheric applications, enlarged version for atmospheric applications. The 10th HITRAN Database Conference, Harvard-Smithsonian Center for Astrophysics, 22-24 June 2008, Cambridge, MA, USA, 2008.

[29] Lodi L, Tennyson J. Line lists for H_2 ^{18}O and H_2 ^{17}O based on empirically-adjusted line positions and ab initio intensities. J Quant Spectrosc Radiat Transf 2012;113:850–858.

[30] Tennyson J, Kostin MA, Barletta P, Harris GJ, Polyansky OL, Ramanlal J, et al. DVR3D: a program suite for the calculation of rotation-vibration spectra of triatomic molecules. Comput Phys Commun 2004;163:85–116.

[31] Tennyson J. TRIATOM, SELECT and ROTLEV – for the calculation of ro-vibrational levels of triatomic molecules. Comput Phys Commun 1986;42:257–270.

[32] Sutcliffe BT, Miller S, Tennyson J. An effective computational approach to the calculation of vibration-rotation spectra of triatomic molecules. Comput Phys Commun 1988;51:73–82.

[33] Sutcliffe BT, Tennyson J. A general treatment of vibration-rotation coordinates for triatomic molecules. Intern J Quantum Chem 1991;39:183–196.

[34] Audi G, Wapstra AH. The 1995 update to the atomic mass evaluation. Nucl Phys A 1995;595:409–480. http://dx.doi.org/10.1016/0375-9474(95)00445-9.

Please cite this article as: Zak EJ, et al. Room temperature linelists for CO_2 asymmetric isotopologues with *ab initio* computed intensities. J Quant Spectrosc Radiat Transfer (2017), http://dx.doi.org/10.1016/j.jqsrt.2017.01.037

[35] Laraia AL, Gamache RR, Lamouroux J, Gordon IE, Rothman LS. Total internal partition sums to support planetary remote sensing. Icarus 2011;215:391–400. http://dx.doi.org/10.1016/j.icarus.2011.06.004.

[36] Johns JWC. Absolute intensity and pressure broadening measurements of CO_2 in the 4.3-μm region. J Mol Spectrosc 1987;125:442–464. http://dx.doi.org/10.1016/0022-2852(87)90109-3.

[37] Johns JWC, Vander Auwera J. Absolute intensities in CO_2: the ν_2 fundamental near 15 μm. J Mol Spectrosc 1990;140:71–102. http://dx.doi.org/10.1016/0022-2852(90)90008-e.

[38] Teffo J-L, Daumont L, Claveau C, Valentin A, Tashkun SA, Perevalov VI. Infrared spectra of the $^{16}O^{12}C^{17}O$ and $^{16}O^{12}C^{18}O$ species of carbon dioxide: the region 500–1500 cm^{-1}. J Mol Spectrosc 2002;213:145–152. http://dx.doi.org/10.1006/jmsp.2002.8561.

[39] Toth R, Miller C, Brown L, Devi VM, Benner DC. Line positions and strengths of $^{16}O^{12}C^{18}O$, $^{18}O^{12}C^{18}O$ and $^{17}O^{12}C^{18}O$ between 2200 and 7000 cm^{-1}. J Mol Spectrosc 2007;243:43–61. http://dx.doi.org/10.1016/j.jms.2007.03.005.

[40] Kshirsagar RJ, Giver LP, Chackerian C, Brown LR. The rovibrational intensities of the $2\nu_3$ band of at 4639 cm^{-1}. J Quant Spectrosc Radiat Transf 1999;61:695–701. http://dx.doi.org/10.1016/s0022-4073(98)00058-2.

[41] Toth RA. Line positions and strengths of CO_2 in the 1200–1430 cm^{-1} region. Appl Opt 1985;24:261. http://dx.doi.org/10.1364/ao.24.000261.

[42] Teffo J-L, Daumont L, Claveau C, Valentin A, Tashkun S, Perevalov V. Infrared spectra of the and species of carbon dioxide: II. the 1500-3000 cm^{-1} region. J Mol Spectrosc 2003;219:271–281. http://dx.doi.org/10.1016/s0022-2852(03)00057-2.

[43] Rinsland CP, Benner DC. Absolute intensities of spectral lines in carbon dioxide bands near 2050 cm^{-1}. Appl Opt 1984;23:4523. http://dx.doi.org/10.1364/ao.23.004523.

[44] Claveau C, Teffo J-L, Hurtmans D, Valentin A, Gamache R. Line positions and absolute intensities in the laser bands of carbon-12 oxygen-17 isotopic species of carbon dioxide. J Mol Spectrosc 1999;193:15–32. http://dx.doi.org/10.1006/jmsp.1998.7704.

[45] Devi VM, Rinsland CP, Benner DC. Absolute intensity measurements of CO_2 bands in the 2395–2680-cm^{-1} region. Appl Opt 1984;23:4067. http://dx.doi.org/10.1364/ao.23.004067.

[46] Rinsland CP, Benner DC, Devi VM. Measurements of absolute line intensities in carbon dioxide bands near 52 μm. Appl Opt 1985;24:1644. http://dx.doi.org/10.1364/ao.24.001644.

[47] Claveau C, Teffo J-L, Hurtmans D, Valentin A. Infrared fundamental and first hot bands of (OCO) - $O^{12}C^{17}O$ isotopic variants of carbon dioxide. J Mol Spectrosc 1998;189:153–195. http://dx.doi.org/10.1006/jmsp.1998.7546.

[48] Toth R, Miller C, Brown L, Devi VM, Benner DC. Line strengths of $^{16}O^{13}C^{16}O$, $^{16}O^{13}C^{18}$, $^{16}O^{13}C^{17}O$ and $^{18}O^{13}C^{18}O$, between 2200 and 6800 cm^{-1}. J Mol Spectrosc 2008;251:64–89. http://dx.doi.org/10.1016/j.jms.2008.01.009.

[49] Wunch D, Wennberg PO, Toon GC, Connor BJ, Fisher B, Osterman GB, et al. A method for evaluating bias in global measurements of CO_2 total columns from space. Atmos Chem Phys 2011;11:12317–12337. http://dx.doi.org/10.5194/acp-11-12317-2011.

[50] Lamouroux J, Tran H, Laraia AL, Gamache RR, Rothman LS, Gordon IE, et al. Updated database plus software for line-mixing in CO_2 infrared spectra and their test using laboratory spectra in the 1.5–2.3 μm region. J Quant Spectrosc Radiat Transf 2010;111:2321–2331. http://dx.doi.org/10.1016/j.jqsrt.2010.03.006.

Please cite this article as: Zak EJ, et al. Room temperature linelists for CO_2 asymmetric isotopologues with *ab initio* computed intensities. J Quant Spectrosc Radiat Transfer (2017), http://dx.doi.org/10.1016/j.jqsrt.2017.01.037